AAV Gene Transfer with Tandem Promoter Design Prevents Anti-transgene Immunity and Provides Persistent Efficacy in Neonate Pompe Mice

Pasqualina Colella, Pauline Sellier, Helena Costa Verdera, Francesco Puzzo, Laetitia van Wittenberghe, Nicolas Guerchet, Nathalie Danièle, Bernard Gjata, Solenne Marmier, Severine Charles, et al.

▶ **To cite this version:**

Pasqualina Colella, Pauline Sellier, Helena Costa Verdera, Francesco Puzzo, Laetitia van Wittenberghe, et al.. AAV Gene Transfer with Tandem Promoter Design Prevents Anti-transgene Immunity and Provides Persistent Efficacy in Neonate Pompe Mice. Molecular Therapy - Methods and Clinical Development, 2018, 12, pp.85-101. 10.1016/j.omtm.2018.11.002 . hal-02087558

HAL Id: hal-02087558

https://hal.sorbonne-universite.fr/hal-02087558

Submitted on 2 Apr 2019

HAL is a multi-disciplinary open access archive for the deposit and dissemination of scientific research documents, whether they are published or not. The documents may come from teaching and research institutions in France or abroad, or from public or private research centers.

L'archive ouverte pluridisciplinaire **HAL**, est destinée au dépôt et à la diffusion de documents scientifiques de niveau recherche, publiés ou non, émanant des établissements d'enseignement et de recherche français ou étrangers, des laboratoires publics ou privés.

Molecular Therapy
Methods & Clinical Development
Original Article

AAV Gene Transfer with Tandem Promoter Design Prevents Anti-transgene Immunity and Provides Persistent Efficacy in Neonate Pompe Mice

Pasqualina Colella,[1] Pauline Sellier,[1,2] Helena Costa Verdera,[1,2] Francesco Puzzo,[1] Laetitia van Wittenberghe,[1] Nicolas Guerchet,[1] Nathalie Daniele,[1] Bernard Gjata,[1] Solenne Marmier,[2] Severine Charles,[1] Marcelo Simon Sola,[1] Isabella Ragone,[1] Christian Leborgne,[1] Fanny Collaud,[1] and Federico Mingozzi[1,2,3]

[1]Genethon, INSERM U951 Integrare, University of Evry, Université Paris-Saclay, 91002, Evry, France; [2]University Pierre and Marie Curie Paris 6 and INSERM U974, 75651, Paris, France; [3]Spark Therapeutics, Philadelphia, PA 19103, USA

Hepatocyte-restricted, AAV-mediated gene transfer is being used to provide sustained, tolerogenic transgene expression in gene therapy. However, given the episomal status of the AAV genome, this approach cannot be applied to pediatric disorders when hepatocyte proliferation may result in significant loss of therapeutic efficacy over time. In addition, many multi-systemic diseases require widespread expression of the therapeutic transgene that, when provided with ubiquitous or tissue-specific non-hepatic promoters, often results in anti-transgene immunity. Here we have developed tandem promoter monocistronic expression cassettes that, packaged in a single AAV, provide combined hepatic and extra-hepatic tissue-specific transgene expression and prevent anti-transgene immunity. We validated our approach in infantile Pompe disease, a prototype disease caused by lack of the ubiquitous enzyme acid-alpha-glucosidase (GAA), presenting multi-systemic manifestations and detrimental anti-GAA immunity. We showed that the use of efficient tandem promoters prevents immune responses to GAA following systemic AAV gene transfer in immunocompetent Gaa−/− mice. Then we demonstrated that neonatal gene therapy with either AAV8 or AAV9 in Gaa−/− mice resulted in persistent therapeutic efficacy when using a tandem liver-muscle promoter (LiMP) that provided high and persistent transgene expression in non-dividing extra-hepatic tissues. In conclusion, the tandem promoter design overcomes important limitations of AAV-mediated gene transfer and can be beneficial when treating pediatric conditions requiring persistent multi-systemic transgene expression and prevention of anti-transgene immunity.

INTRODUCTION

In vivo gene therapy with adeno-associated-virus (AAV) vectors has the potential to provide sustained correction of human genetic diseases, as supported by the approval of two AAV-based drugs[1,2] and many ongoing clinical trials. However, the ability to achieve therapeutic levels of transgene expression in multiple affected tissues concomitant with transgene immune tolerance represents an important goal for the field.[3–5] Hepatic restricted AAV-mediated gene transfer has been successfully exploited to achieve this goal with a variety of therapeutic transgenes.[3,6–12] However, hepatocyte-restricted gene transfer is significantly limited under conditions of hepatocyte proliferation, such as the growing liver of an infant, because of loss of episomal AAV genomes.[13–18] This hampers application of this strategy to severe congenital diseases requiring therapeutic gene delivery early in life.[14–17] In addition, extra-hepatic expression of the therapeutic transgene is needed to treat diseases caused by mutation in body-wide expressed genes encoding for non-secreted proteins. To date, this has been pursued using promoters driving expression of the therapeutic transgene, either constitutively[19–23] or in affected tissues,[24–27] although gene transfer to extra-hepatic tissues, such as muscle and the CNS, can sometimes result in enhanced anti-transgene immunogenicity.[5,7,21–23,25–36]

Pompe disease (PD; OMIM: #232300) is a prototype model of infantile neuromuscular pathology in which treatment is complicated by detrimental immune responses to the therapeutic protein.[37] PD is a multi-systemic pathology presenting with severe neuromuscular manifestations caused by lack of acid-alpha-glucosidase (GAA), a lysosomal enzyme that hydrolyzes glycogen to glucose.[37] *GAA* is ubiquitously expressed, and its deficiency causes whole-body accumulation of glycogen,[37] resulting in hepatomegaly, cardiomegaly, progressive muscle weakness, and respiratory insufficiency.[37] Effective treatment of PD requires restoration of GAA enzyme activity in virtually all tissues,[38] concomitant with the prevention of anti-GAA immunity.[7,28,30,37–43] Additionally, early intervention is crucial for

Received 11 September 2018; accepted 12 November 2018;
https://doi.org/10.1016/j.omtm.2018.11.002.

Correspondence: Pasqualina Colella, Genethon, INSERM U951 Integrare, University of Evry, Université Paris-Saclay, 91002, Evry, France.
E-mail: pcolella@genethon.fr
Correspondence: Federico Mingozzi, Genethon, INSERM U951 Integrare, University of Evry, Université Paris-Saclay, 91002, Evry, France.
E-mail: fmingozzi@genethon.fr

This is an open access article under the CC BY-NC-ND license (http://creativecommons.org/licenses/by-nc-nd/4.0/).

successful treatment, particularly for the severe infantile-onset PD form (IOPD).[39–45] Enzyme replacement therapy (ERT) with recombinant human GAA is used to treat PD; however, inefficient cross-correction of skeletal muscle and the CNS[38] and anti-GAA immunity[39–43] severely impair the efficacy of the approach. Anti-GAA immunity is also a concern for AAV-mediated gene therapy for PD. For instance, anti-GAA antibodies have been observed in a phase I–II clinical trial for IOPD upon *GAA* muscle gene transfer using the ubiquitous cytomegalovirus (CMV) promoter.[20] Similarly, strong humoral anti-GAA immune responses are observed in a mouse model of PD when using both ubiquitous and muscle-specific promoters.[7,25,28–30,46,47]

Here we developed a novel tandem promoter expression cassette design that resulted in combined hepatic and extrahepatic tissue-specific transgene expression and prevented anti-transgene immune responses when used in the context of systemic AAV gene therapy. Tandem promoters were developed by rational design through multiplexing of selected tissue-specific regulatory elements widely reported to be active in hepatocytes,[48,49] muscle,[50] and neurons.[51–53] The efficacy of AAV gene therapy using the tandem promoters was validated in the mouse model of PD. Here we showed that systemic AAV gene delivery using transgene expression cassettes under the control of liver-muscle and liver-neuron tandem promoters allowed to achieve simultaneously hepatic and extra-hepatic transgene expression and to prevent anti-GAA immune responses in immunocompetent mice. Importantly, concomitant transgene expression in liver and muscle using the most efficient tandem promoter resulted in persistent therapeutic GAA expression in neonate Gaa−/− mice treated systemically with AAV-*GAA* vectors.

This work addresses crucial limitations of AAV vector-mediated gene transfer for systemic multi-organ diseases characterized by early severe phenotype.

RESULTS

Rational Design of Tandem Promoters to Obtain Simultaneous Hepatic and Extra-hepatic Transgene Expression

We hypothesized that, by multiplexing different tissue-specific promoter elements, we could express a therapeutic transgene in both hepatic and extra-hepatic disease target tissues. To meet this goal, we identified, in the literature, tissue-specific regulatory elements[6,51,54–56] that could be combined in a transgene expression cassette, respecting the AAV genome size limitation (<5 kb).[57] To provide strong tolerogenic hepatic transgene expression, we selected the Apolipoprotein E enhancer and the human alpha-1 anti-trypsin promoter elements (Figure 1A; Figure S1),[6,48,54] also reported to minimize the risk of genotoxicity.[58] To achieve transgene expression in muscle, we selected the short synthetic spC5.12 promoter (C5.12),[55,56] which is active in both cardiac and skeletal muscle (type I and II fibers) and has been successfully used in large animal models of muscular dystrophy (Figure 1A; Figure S1).[50] For transgene expression in the CNS, we selected the pan-neuron human synapsin promoter (hSYN; Figure 1A; Figure S1) because it has been reported to be neuron-specific in both the brain and spinal cord in small and large animal models.[51–53] Based on this, we used the full sequence of each tissue-specific promoter to generate three tandem promoters: the enhanced C5.12 promoter (Enh.C5.12, Apolipoprotein E [ApoE]-C5.12), the full liver-muscle promoter (LiMP, ApoE-hAAT-C5.12), and the full liver-neuron promoter (LiNeuP, ApoE-hAAT-hSYN) (Figure 1A). The tandem promoters Enh.C5.12 and LiMP were generated for concomitant transgene expression in liver and muscle, whereas LiNeuP was generated to drive transgene co-expression in liver and neurons (Figure 1A). In the tandem promoters, the ApoE-hAAT sequences were positioned upstream of the additional promoter elements based on the reported low transactivation activity in case of AAV integration in the genomic DNA.[58] As controls for the specificity and the potency of the tandem promoters, we generated expression cassettes containing either the single-tissue promoters (hAAT, C5.12, hSYN; Figure S1) or the strong ubiquitous CAG promoter (Figure S1).[59] All promoters were cloned in expression cassettes encoding a codon-optimized human *GAA* transgene (*hGAA*) and flanked by the AAV inverted terminal repeats (ITRs) for vector packaging (Figure 1A; Figure S1). We used two *hGAA* transgenes we recently described:[47] one encoding for the native GAA enzyme (hGAA) and one for a secretable GAA enzyme (sec-hGAA). The resulting size of the expression cassettes was less than 5 kb (Figure 1A). Because we previously reported that sec-hGAA is endowed with lower immunogenicity and superior therapeutic efficacy than the native hGAA form,[47,60,61] the latter was specifically used to evaluate anti-transgene immune responses, whereas sec-hGAA was used in disease rescue experiments.

Tandem Liver-Muscle and Liver-Neuron Promoters Drive Transgene Expression in the Desired Cell Lines

We tested the activity of the tandem promoters in different cell lines by transient transfection of plasmids encoding the sec-hGAA (Figures 1B–1I). We evaluated the ability of the tandem liver-muscle promoters Enh.C5.12 and LiMP to drive *sec-hGAA* expression in both hepatocyte and muscle cell lines (Figure 1B–1E). In HuH7 hepatocyte cells, LiMP showed significantly higher activity compared with both the C5.12 and EnhC5.12 promoters (Figures 1B and 1D; Figure S2A). In C2 myoblasts, both LiMP and Enh.C5.12 showed significantly higher activity compared with the C5.12 and the hAAT promoters (Figures 1C and 1E; Figure S2B). These features make LiMP a candidate for strong combined liver-muscle transgene expression and EnhC5.12 a strong muscle promoter with a slightly higher liver-transcriptional activity than C5.12 (Figures 1B–1E; Figures S2A and S2B). The increased activity of the Enh.C5.12 promoter and LiMP versus C5.12 alone in muscle cells (Figures 1C and 1E; Figure S2B) highlights a synergy between the liver and muscle regulatory elements, resulting in enhanced transgene expression in muscle.

We next evaluated the ability of LiNeuP (Figure 1A; Figure S1) to drive *sec-hGAA* expression in both hepatocyte and neuronal cell lines (Figures 1F–1I; Figures S2C and S2D). We transiently transfected

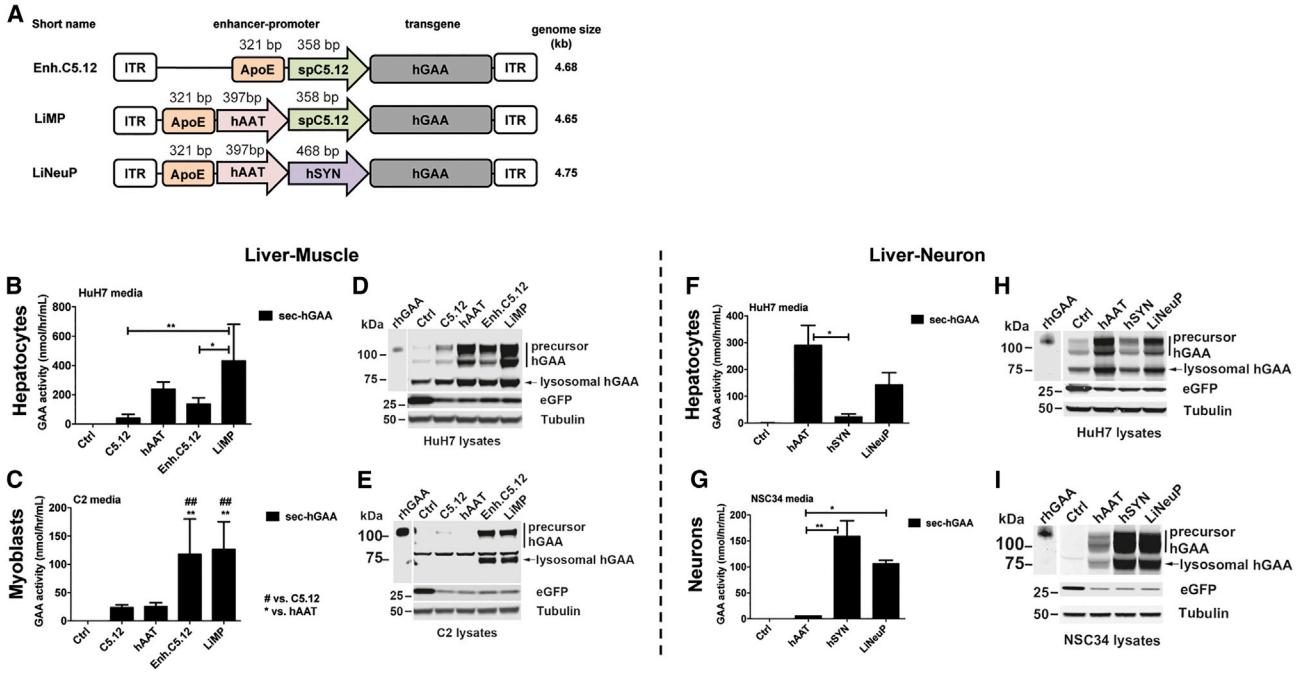

Figure 1. Tandem Promoter Design and Transcriptional Specificity in Cell Lines

(A) Tandem promoter design. The tandem promoters generated were the enhanced C5.12 promoter (Enh.C5.12), composed of the liver ApoE enhancer and the muscle C5.12 promoter; the full liver-muscle promoter LiMP, composed of the liver ApoE enhancer, the hAAT promoter, and the muscle C5.12 promoter; and the liver-neuron promoter LiNeuP, composed of the liver ApoE enhancer, the hAAT promoter, and the neuron hSYN promoter. The size of the enhancer-promoter elements and of the AAV genome, including ITRs, is depicted. ITR, inverted terminal repeat for AAV packaging; ApoE, Apolipoprotein E enhancer; hAAT, human alpha-1 anti-trypsin promoter; spC5.12, synthetic promoter C5.12; hSYN, human Synapsin promoter; hGAA, codon-optimized human acid-alpha-glucosidase transgene encoding for either the native (hGAA) or secretable (sec-hGAA) enzyme. (B–I) Analysis of transgene expression 72 hr after transient transfection of HuH7 human hepatocyte cells (B, D, F, and H), C2 myoblast cells (C and E), or NSC34 neuron cells (G and I) with plasmids encoding sec-hGAA under the control of Enh.C5.12 and LiMP and LiNeuP. Plasmids encoding sec-hGAA under the control of the muscle-specific (C5.12), hepatocyte-specific (hAAT), and neuron-specific (hSYN) promoters (Figure S1) were used for comparison. A plasmid encoding EGFP was used as a negative control (Ctrl) and co-transfected with *sec-hGAA*-expressing plasmids as a positive control for transfection. (B, C, F, and G) GAA activity in cell media at 72 hr; data are depicted as average ± SD of n = 4 (B and C) or n = 2 (F and G) independent experiments. Statistical analysis was performed by two-way ANOVA (promoter, replicate) with Tukey *post hoc*. *$p < 0.05$, **$p < 0.01$, ##$p < 0.01$. (D, E, H, and I) Representative western blot analysis of cell lysates with anti-human GAA antibody. Anti-EGFP and anti-tubulin antibodies were used as a transfection control and loading control, respectively. The molecular weight marker (kilodaltons) is depicted. The pictures are representative of n = 2 independent experiments. Western blot quantification is depicted in Figures S2A–S2D.

HuH7 hepatocyte cells and NSC34 neuronal cells (Figures 1F–1I; Figures S2C and S2D).[62] In hepatocytes, LiNeuP provided higher enzyme activity in media (Figure 1F) and significantly higher protein amount in lysates (Figure 1H; Figure S2C) compared with hSYN alone. In neuronal cells, LiNeuP led to significantly higher enzyme activity (Figure 1G) and high GAA protein expression in cell lysates compared with the hepatocyte-specific hAAT promoter (Figure 1I; Figure S2D).

The specificity of the tandem liver-muscle and liver-neuron promoters was further confirmed by the low activity observed in non-target cells compared with the ubiquitous CAG promoter (Figures S2E and S2F).

Overall, these results indicate that LiMP is an ideal candidate for liver and muscle transgene co-expression, whereas LiNeuP drives efficient transgene expression in both hepatocyte and neuronal cells.

Systemic AAV Gene Delivery Using LiMP and LiNeuP Results in Selective Transgene Expression in Target Mouse Tissues

Based on the *in vitro* results, we then assessed the ability of the newly generated tandem promoters Enh.C5.12, LiMP, and LiNeuP to drive multi-tissue transgene expression in *in vivo* following AAV gene transfer (Figure 2). AAV vectors encoding native hGAA under the control of the tandem promoters were injected systemically into 6-week-old wild-type C57BL/6 mice for transgene expression analysis (Figures 2A–2F). For comparison, we produced AAV vectors encoding *hGAA* under the control of the ubiquitous CAG promoter or single tissue-specific promoters (hAAT, C5.12, and hSYN) (Figures 2A–2F). We selected AAV serotype 9 based on its broad tropism for liver, cardiac muscle, skeletal muscle, and neurons.[63–65] One month after intravenous injection of AAV9-*hGAA* vectors at a dose of 2×10^{12} vector genomes (VG)/kg, we collected liver, cardiac muscle (heart), skeletal muscle (quadriceps), spinal cord, and brain to evaluate *hGAA* mRNA expression by qRT-PCR (Figures 2A–2F).

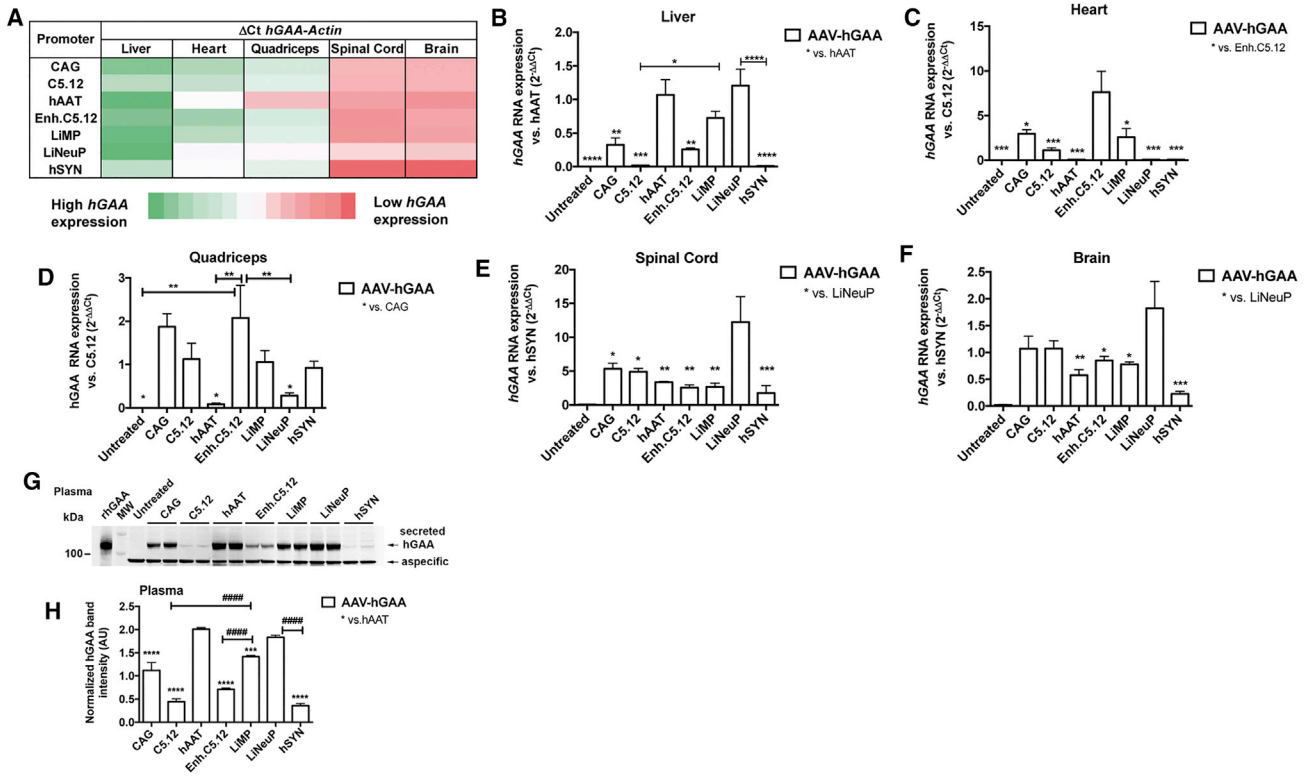

Figure 2. Transcriptional Activity of Tandem Promoters *In Vivo* following Systemic Delivery of AAV-*hGAA* Vectors

(A–H) Analysis of *hGAA* transgene mRNA expression in tissues (A–F) and hGAA protein expression in plasma (G and H) of 3-month-old C57BL/6 mice 6 weeks following intravenous injection of AAV9 vectors (dose, 2×10^{12} vg/kg) harboring codon-optimized human GAA transgene (hGAA, encoding for the native enzyme) under the control of tandem promoters (Enh.C5.12, LiMP, LiNeuP) or the ubiquitous (CAG), hepatocyte-specific (hAAT), and muscle-specific (C5.12) promoters for comparison. Untreated C57BL/6 mice were used as a negative control; n = 4 mice/cohort. (A) Heatmap showing the expression of the *hGAA* transgene mRNA normalized by the expression of the endogenous mouse *Actin* gene (ΔCt) in the tissue analyzed and determined by qRT-PCR. (B–F) Relative expression (fold change) of the *hGAA* transgene mRNA in tissues. The fold change transgene expression is depicted in comparison with control tissue-specific promoters: hAAT for liver (B), C5.12 for heart (C) and quadriceps (D), and hSYN for spinal cord (E) and brain (F). (B–F) Data are depicted as average ± SD. (G) Representative western blot analysis of mouse plasma with anti-human GAA antibody. The molecular weight marker (kilodaltons) is depicted. rhGAA, recombinant human GAA loaded as a positive control. (H) Quantification of the hGAA protein band in plasma normalized by the aspecific band. Data are depicted as average ± SD of n = 4 mice/cohort. (B–F and H) Statistical analysis; one-way ANOVA with Tukey *post hoc*. Asterisks on the bars show significant differences versus mouse cohorts specified in the legend. (B–H) *p < 0.05, **p < 0.01, ***p < 0.001, ****p < 0.0001, ####p < 0.0001.

As reported in other studies,[63,64,66] higher VG copy numbers (VGCNs; ****p < 0.001 liver versus all tissues; Figure S3A) and transgene mRNA levels (Figure 2A) were found in liver, followed by heart, skeletal muscle, and nervous system. We then analyzed the *hGAA* mRNA fold change expression in each tissue in comparison with the respective control promoters (Figures 2B–2F). In the liver, significantly higher transgene expression was achieved with LiMP compared with C5.12 and LiNeuP compared with hSYN (Figure 2B). The activity of the tandem promoters LiMP and LiNeuP in the liver was not significantly different from that of the hAAT promoter (Figure 2B). Lower liver transgene expression was instead observed using the tandem Enh.C5.12 promoter compared with hAAT (Figure 2B). In cardiac and skeletal muscle, high transgene expression was observed using the tandem Enh.C5.12 promoter and LiMP (Figures 2A, 2C, and 2D). Enh.C5.12 was significantly more active than LiMP and C5.12 in heart (Figure 2C). In skeletal muscle (Figure 2C), the activity of the tandem Enh.C5.12 promoter and LiMP was higher than hAAT and not significantly different compared with control C5.12 and strong ubiquitous CAG promoters. Notably, LiMP drove transgene expression in both liver (Figure 2B) and muscle (Figures 2C and 2D) at levels that were not significantly different from the single hAAT and C5.12 promoters, respectively. In liver, LiMP also showed markedly higher activity than Enh.C5.12.

In the CNS, the overall *hGAA* mRNA expression was low compared with liver and muscle (Figure 2A), as expected from AAV9 vector biodistribution in adult mice (Figure S3A).[63] Despite this, the highest transgene hGAA transgene expression in both spinal cord and brain was driven by LiNeuP (Figures 2E and 2F). The slight, not significant increase in transgene expression observed using the other promoters compared with hSYN (Figures 2E and 2F) could possibly derive from some low transcriptional activity and/or mRNA transport from the

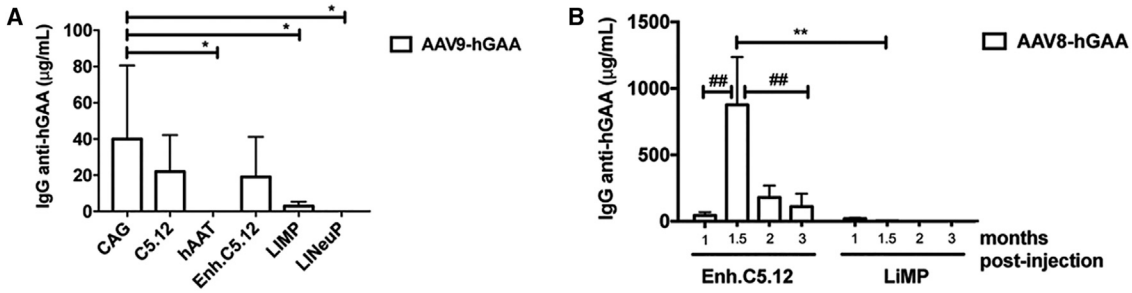

Figure 3. Anti-hGAA Humoral Immune Responses in Gaa–/– Mice following AAV Gene Transfer of hGAA Using Tandem Promoters

(A) Analysis of anti-hGAA antibodies (immunoglobulin G [IgG]) in Gaa−/− mice at 1.5 months following intravenous injection of AAV9 vectors (dose, 2×10^{12} vg/kg) harboring a codon-optimized hGAA transgene encoding for the native enzyme under the control of tandem promoters (Enh.C5.12, LiMP, LiNeuP) or the ubiquitous (CAG), hepatocyte-specific (hAAT), and muscle-specific (C5.12) promoters for comparison. Gaa−/− mice were treated at 3 months of age. Data are depicted as average ± SD; n = 5 mice/cohort. Statistical analysis: one-way ANOVA with Tukey *post hoc*. (B) Analysis of anti-hGAA IgGs in Gaa−/− mice 1, 1.5, 2, and 3 months following intravenous injection of AAV8-*hGAA* vectors (native hGAA; dose, 2×10^{12} vg/kg) harboring Enh.C5.12 and LiMP promoters. Gaa−/− mice were treated at 3–4 months of age. Data are depicted as average ± SD; n = 3–5 mice/cohort. EnhC5.12: n = 5 at 1, 1.5, and 2 months; n = 4 at 3 months. LiMP: n = 4 at 1, 1.5, and 2 months; n = 3 at 3 months. Statistical analysis: two-way ANOVA (promoters, time) with Sidak *post hoc*, significant differences are indicated by asterisks. Two-way ANOVA (time) with Tukey *post hoc*, significant differences are indicated by hash marks. *$p < 0.05$, **$p < 0.01$, ##$p < 0.01$.

main transduced tissue (e. g. liver, muscle).[67] Notably, the ability of LiNeuP to drive efficient transgene expression in both liver (Figure 2B) and CNS (Figures 2E and 2F) compared with hAAT and hSYN confirms its dual transcriptional activity.

Finally, compared with the ubiquitous CAG promoter (Figures 2B–2E), tandem promoters showed preserved tissue specificity. LiMP-driven expression in neurons was limited and not different from the hAAT and C5.12 promoters (Figures 2E and 2F), whereas LiNeuP-driven expression in muscle was not different from that of hAAT and hSYN promoters (Figures 2C and 2D).

The specificity of the most efficient liver-muscle and liver-neuron promoters was confirmed by the low or absent activity observed in non-target tissues, such as kidney, lung, and spleen (Figures S3B and S3C). In the lungs, some detectable *hGAA* mRNA expression observed using the LiMP could possibly derive from promoter activity in smooth muscle cells (Figure S3B). As expected,[63,64,66] vector genome copy numbers (VGCNs) were higher in liver compared with other tissues (Figures S3D and S3E).

Overall, the *hGAA* mRNA expression data show that the tandem promoters LiMP and LiNeuP drive efficient and specific transgene expression in target tissues (Figures 2A–2F; Figures S3B and S3C).

Next we quantified hGAA protein in the plasma of C57BL/6 mice injected with the AAV9-*hGAA* vectors. One month after treatment, western blot analyses of mouse plasma showed that the amount of circulating hGAA was higher using LiMP compared with C5.12 and Enh.C5.12, and LiNeuP compared with hSYN (Figures 2G and 2H). The control hAAT promoter provided the highest amount of circulating hGAA compared with the other promoters (Figures 2G and 2H). These data demonstrate that LiMP and LiNeuP drive efficient *hGAA* transgene expression in hepatic tissues and target extra-hepatic tissues (Figures 2A–2F) while also providing a high amount of circulating hGAA (Figures 2G and 2H) to mediate cross-correction via tissue uptake.

Tandem Promoters with Strong Liver Activity Prevent the Development of Immune Responses to hGAA in Gaa–/– Mice

Gene transfer of native *hGAA* to Gaa−/− mice driven by either ubiquitous or muscle-specific promoters has been reported to induce unwanted humoral immune responses toward the hGAA protein.[25,28–30,46,47] Conversely, we[47,68] and others[7,46] have shown that restriction of native *hGAA* transgene expression to hepatocytes prevents the development of anti-hGAA immunity and provides stable immunological tolerance to the transgene product. To evaluate the immunological properties of the tandem liver-muscle and liver-neuron promoters, we delivered AAV9 vectors encoding native hGAA systemically to adult immunocompetent Gaa−/− mice (vector dose, 2×10^{12} vg/kg) and evaluated anti-hGAA humoral immune responses (Figure 3A). Adult Gaa−/− mice were specifically used in these experiments because neonate animals have been reported to be more prone to develop pro-tolerogenic responses.[69–71] At early time points after treatment, high anti-hGAA immunoglobulin G (IgG) was induced in mice treated with the Enh.C5.12 vector in addition to the control CAG and C5.12 vectors (Figure 3A). Conversely, anti-hGAA IgG measured in mice treated with LiMP, LiNeuP, and control hAAT vectors (Figure 3A) was either low or absent and significantly different from that measured in the CAG cohort (Figure 3A). The use of the tandem promoters LiMP and LiNeuP prevented the induction of anti-hGAA IgG long-term (Figure S4A). Conversely, anti-hGAA IgG peaked with time in the C5.12 cohort, leading to significantly higher levels than those measured in the other cohorts (Figure S4A). Interestingly, these data suggest that liver transgene expression determined by the CAG and Enh.C5.12 promoters may reduce but not prevent anti-hGAA humoral immune responses (Figure 3A; Figure S4A). VGCN showed no important impact of genome

sequence on liver transduction (Figure S4B). Consistent with our previous findings using AAV gene transfer of native hGAA,[47] no significant recovery of muscle strength was observed 3 and 5 months after AAV treatment at the vector dose tested (Figures S4C and S4D).

Next we used AAV8 vectors, which efficiently target mouse liver in addition to muscle,[63,65] to further compare the immunological properties of gene transfer with the tandem liver-muscle Enh.C5.12 and LiMP promoters (Figure 3B). Anti-hGAA IgG was readily detected when using the Enh.C5.12 promoter, with a peak 6 weeks after vector delivery followed by a significant decrease at later time points (Figure 3B). No or low antibodies against the hGAA transgene product were instead detected when using LiMP at any of the time points analyzed (Figure 3B). At sacrifice, the amount of the hGAA protein measured in liver by western blot showed higher transgene expression in mice treated with AAV8-LiMP vectors compared with those treated with AAV8-Enh.C5.12 vectors (Figures S5A and S5B). These findings are in agreement with previously published work showing that immune tolerance positively correlates with antigen expression levels in the liver.[6,72] No significant differences in hGAA content were observed in quadriceps of AAV8-treated mice (Figures S5C and S5D). Analysis of VGCN in liver and quadriceps also showed no significant differences among the vectors used (Figures S5E and S5F).

Next, being muscle a highly immunogenic tissue,[29,36] we tested whether AAV gene transfer using LiMP could decrease a pre-existing anti-transgene humoral immune response. To this aim, we immunized Gaa−/− mice with three intravenous injections of rhGAA at a dose of 20 mg/kg (Figure S6A). Then, 2 weeks later, we measured anti-GAA IgG in plasma and treated the immunized mice with AAV9-LiMP-*hGAA* vectors by intravenous delivery (Figure S6B). An AAV9-hAAT-*hGAA* vector was used as a tolerogenic control.[11,12,68] Six weeks after AAV treatment (at a dose of 2×10^{12} vg/kg), IgG anti-hGAA was significantly decreased in mice treated with LiMP and hAAT vectors but in mice treated with a control AAV vector expressing luciferase (Figure S6B).

Overall, these results indicate that AAV gene transfer with tandem promoters endowed with a strong hepatic expression component, like LiMP, results in efficient prevention of immune responses to the GAA transgene product.

The Tandem Liver-Muscle Promoter LiMP Provides Persistent *GAA* Transgene Expression in Neonate Gaa−/− Mice

Hepatic transgene expression upon AAV gene transfer in neonate animals has been reported to be temporally limited by the loss of episomal vector genomes from dividing hepatocytes during liver growth.[14,15,17] To overcome this limitation, we tested the ability of LiMP, to prevent anti-hGAA immune responses and provide long-term transgene expression in neonate Gaa−/− mice upon systemic AAV injection because of its efficient liver-muscle transcriptional activity. To this aim, we intravenously injected Gaa−/− mice on post-natal days 1–2 with AAV vectors encoding sec-hGAA under the control of LiMP or the single C5.12 and hAAT promoters for comparison (dose, 6×10^{10} vg/pup [3×10^{13} vg/kg]) (Figures 4 and 5; Figures S7 and S8). The AAV8 vector was used because it efficiently targets liver, muscle, and the nervous system.[63,65,73] At the end of the study (3 months after treatment), the amount of therapeutic enzyme in the circulation (Figures 4A and 4B) was higher in Gaa−/− mice treated with hAAT and LiMP compared with C5.12 vectors. In the liver, sec-*hGAA* transgene mRNA expression (Figure S7A), protein content (Figures S7B and S7C), and enzyme activity (Figure S7D) were also higher in mice treated with LiMP and hAAT compared with C5.12 vectors. At the end of the study, immunostaining for sec-hGAA in liver sections confirmed enzyme expression in adult hepatocytes using hAAT and LiMP (Figure 4C). Analysis of VGCN in the liver showed no significant differences among the vectors used (Figure S7E). Loss of AAV genomes over time because of hepatocyte proliferation was indicated by the reduced amounts of circulating sec-hGAA enzyme measured in the plasma 3 months versus 1 month after treatment in the hAAT and LiMP cohorts (Figures S7F and S7G). Interestingly, at the end of the study, GAA activity in muscle (heart, diaphragm, quadriceps, and triceps) was significantly higher in Gaa−/− mice treated with LiMP compared with both hAAT and C5.12 vectors (Figures 4D–4G). GAA activity achieved with LiMP vectors was supra-physiological compared with Gaa+/+ mice (Figures 4D–4G). Expression analyses in diaphragm and triceps also showed significantly higher amounts of sec-hGAA protein (Figures 4H and 4I; Figures S8A and S8B) and mRNA (Figure S8C) in Gaa−/− mice treated with LiMP compared with C5.12 and hAAT. The increased activity of the LiMP promoter in muscle compared with both hAAT and C5.12 alone (Figures 4D–4I; Figures S8A–S8C) highlights the synergy between hepatocyte- and muscle-specific transcriptional elements, resulting in enhanced transgene expression in muscle. Interestingly, the higher expression of sec-hGAA achieved in muscle with LiMP (Figures 4D–4I; Figures S8A–S8C) resulted in higher amounts of circulating enzyme compared with C5.12 but not hAAT (Figures 4A and 4B). One possible explanation is that muscle, differently from liver, does not efficiently secrete proteins into the bloodstream.[74] No significant differences in VGCN were observed in skeletal muscle (Figure S8D).

The sec-hGAA protein was also clearly detected in both spinal cord and brain of AAV-treated Gaa−/− mice compared with untreated Gaa−/− mice (control [Ctrl]; Figures 4J–4M). In the spinal cord, enzyme levels were significantly higher with LiMP compared with C5.12 and hAAT vectors (Figures 4J and 4K). In the brain, LiMP provided a higher amount of hGAA protein compared with C5.12 but not hAAT (Figures 4L–4M). Despite detection of the GAA transgene protein, GAA activity levels in the CNS of AAV-treated Gaa−/− mice was not different from untreated Gaa−/− mice (Ctrl; Figures S8E and S8F), consistent with our previous findings showing the lower sensitivity of the activity assay compared with the western blot assay.[47]

Overall, these results show that the tandem LiMP promoter provides robust and long-lasting transgene expression in both liver and muscle of neonate Gaa−/− mice together with superior enzyme targeting to the spinal cord and brain.

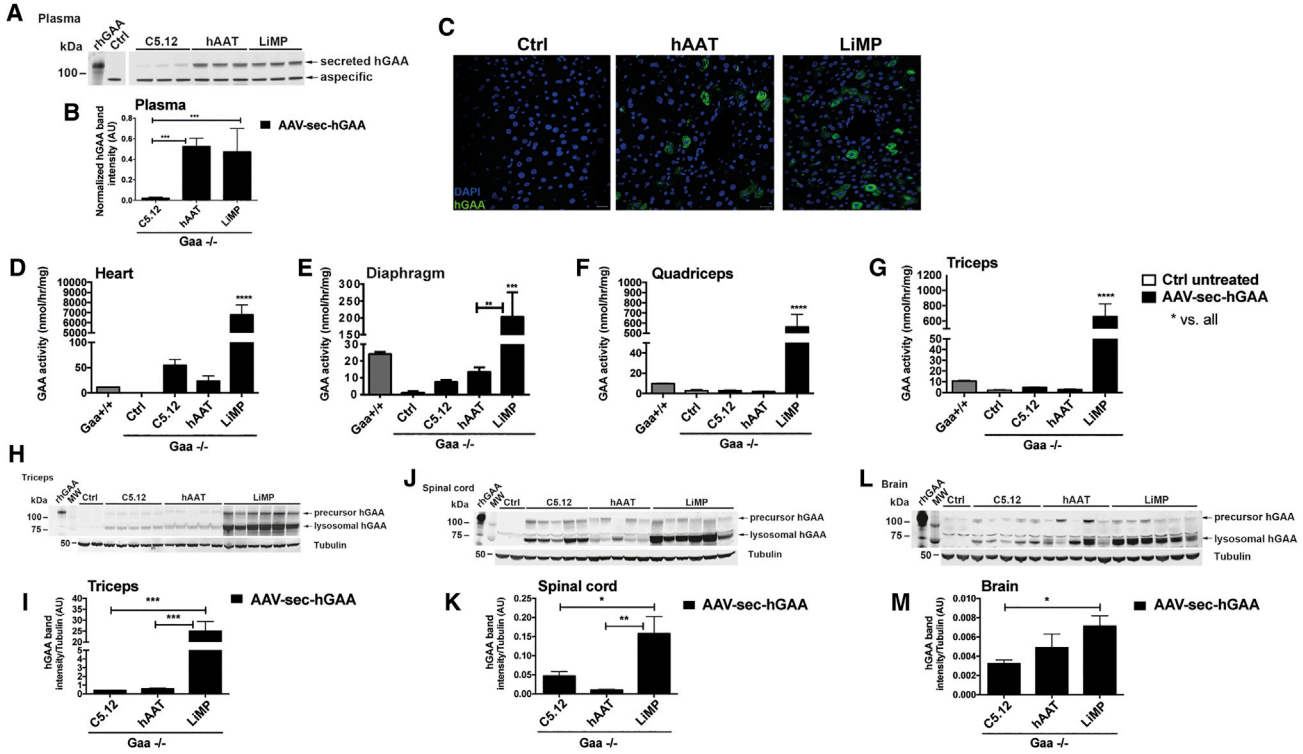

Figure 4. Efficient Expression of *sec-hGAA* following AAV Gene Transfer to Neonate Gaa–/– Mice Using the Tandem LiMP Promoter

(A–M) Analysis of hGAA expression in plasma (A and B) and tissues (C–M) of 3-month old Gaa−/− mice treated as neonates by intravenous injection of AAV8 vectors (dose, 3×10^{13} vg/kg) encoding a codon-optimized sec-hGAA under the control of the tandem promoter LiMP (n = 6) or the muscle-specific (C5.12, n = 5) and hepatocyte-specific (hAAT, n = 5) promoters for comparison. Littermate untreated Gaa−/− mice were used as affected controls (n = 6). Littermate Gaa+/+ mice were used as unaffected controls (n = 8). (A) Representative western blot of Gaa−/− plasma with anti-human GAA antibody. The molecular weight marker (kilodaltons) is depicted. rhGAA was loaded as a positive control. (B) Quantification of the hGAA protein band in Gaa−/− plasma normalized by the aspecific band. (C) Immunofluorescence analyses of liver sections with anti-human GAA antibody. The scale bar represents 20 μm. The pictures are representative of n = 2 (hAAT) or n = 4 (LiMP) AAV-treated Gaa−/− mice and n = 1 untreated Gaa−/− mouse (Ctrl). (D–G) Analysis of GAA enzyme activity in muscle: heart (D), diaphragm (E), quadriceps (F), triceps (G). (H–M) Western blot analyses of Gaa−/− triceps (H and I), spinal cord (J and K), and brain (L and M) with anti-human GAA antibody. Anti-tubulin antibody was used as a loading control. rhGAA was loaded as a positive control. The molecular weight marker (kilodaltons) is depicted. (I, K, and M) Quantification of hGAA protein bands in tissues normalized by tubulin. (B, D–G, I, K, and M) Data are depicted as average ± SD; n = 5–8 mice per cohort as described above. Statistical analysis: one-way ANOVA with Tukey *post hoc*. *p < 0.05, **p < 0.01, ***p < 0.001, ****p < 0.0001. (D–G). Asterisks show significant differences versus all mouse cohorts.

Transgene Expression Driven by LiMP Rescues the Disease Phenotype in Neonate Gaa–/– Mice

Next we measured glycogen content in muscle and the nervous system of Gaa−/− mice treated as neonates. Three months after treatment, pathological glycogen accumulation was significantly reduced in heart (Figure 5A), triceps (Figure 5B), diaphragm (Figure 5C), quadriceps (Figure S8G), spinal cord (Figure S8H), and brain (Figure 5D) of AAV-treated mice compared with untreated Gaa−/− mice (Ctrl). In diaphragm (Figure 5C) and brain (Figure 5D), only hAAT and LiMP vectors, but not C5.12, led to normalization of glycogen accumulation. This observation (Figures 5C and 5D) was consistent with the observed higher amount of therapeutic enzyme provided by LiMP compared with C5.12 in both tissues (Figures 4L and 4M; Figures S8A and S8B). At the end of the study, significant correction of cardiomegaly was found in all AAV-treated mice (Figure 5E). Notably, muscle strength was significantly rescued only in Gaa−/− mice treated with LiMP compared with untreated Gaa−/− mice (Ctrl; Figure 5F). Although humoral immune responses to the vector capsid were readily found in AAV8-treated Gaa−/− mice, no anti-hGAA IgGs were detected at all time points (1, 2, and 3 months after treatment; Table S1).

These results clearly show that AAV-*sec-hGAA* gene therapy with LiMP in neonate Gaa−/− mice results in whole-body enzyme targeting and therapeutic efficacy superior to the C5.12 and hAAT promoters.

LiMP-Driven GAA Transgene Expression Allows Rescue of Neonatal PD at Low Vector Doses

We next tested whether gene transfer with tandem promoters in neonate Gaa−/− mice could result in therapeutic efficacy at low

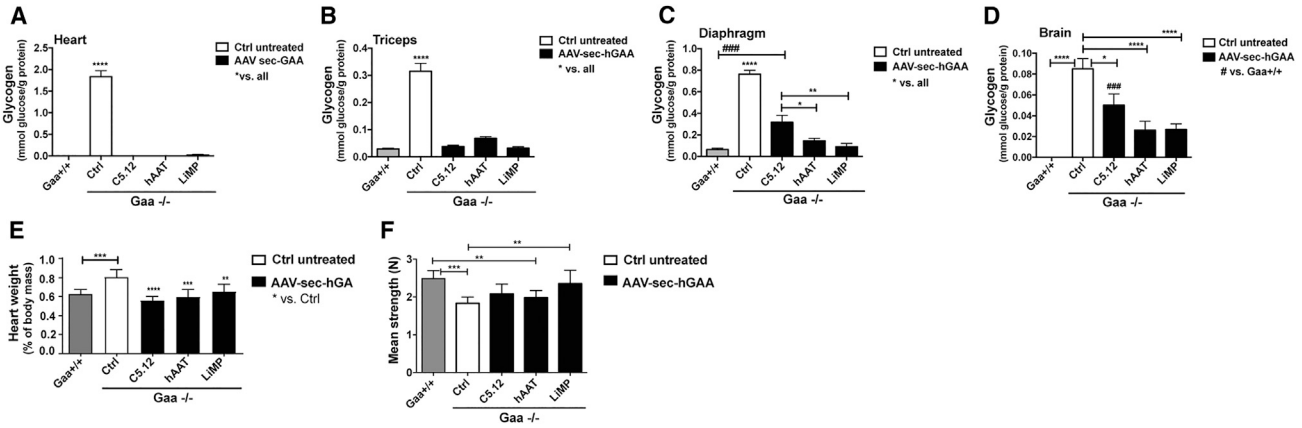

Figure 5. Efficacy in Gaa–/– Mice Treated as Neonates with Systemic AAV Gene Therapy Using the Tandem LiMP Promoter

(A–F) Analysis of glycogen accumulation in tissues (A–D), cardiomegaly (E), and muscle strength (F) in 3-month-old Gaa−/− mice treated as neonates with intravenous injection of AAV8 vectors (dose, 3×10^{13} vg/kg) encoding a codon-optimized sec-hGAA under the control of LiMP (n = 6) or the muscle-specific (C5.12, n = 5) and hepatocyte-specific (hAAT, n = 5) promoters for comparison. Littermate untreated Gaa−/− mice were used as affected controls (n = 6); littermate Gaa+/+ mice were used as unaffected controls (n = 8). (A–D) Glycogen accumulation measured in heart (A), triceps (B), diaphragm (C), and brain (D). (E) Heart weight normalized by body weight. (F) Muscle strength measured by 4-limb grip test. (A–F) Data are depicted as average ± SD; n = 5–8 mice per cohort as described above. Statistical analysis: one-way ANOVA with Tukey *post hoc*. *p < 0.05, **p < 0.01, ***p < 0.001, ****p < 0.0001, ###p < 0.001. (A–E) Asterisks and hash marks on the bars show significant differences versus mouse cohorts specified in the legends.

vector doses. Animals were treated on days 1–2 after birth with 1.2×10^{10} vg/pup (6×10^{12} vg/kg) (Figures 6 and 7; Figures S9 and S10) of vectors expressing *sec-hGAA* under the control of LiMP compared with hAAT. AAV serotype 9 was used to target the liver, muscle, and nervous system.[63–65,75] The amount of circulating GAA enzyme was not different in Gaa−/− mice treated with LiMP and hAAT vectors for the duration of the study (Figures 6A and 6B; Figures S9A and S9B). As observed in the AAV8 study (Figure S7A), transgene mRNA expression in the liver showed no significant differences among the LiMP and hAAT promoters, highlighting their similar hepatic transcriptional activity (Figure S9C). Liver GAA content (Figures S9D and S9E) and activity (Figure S9F) were slightly higher in LiMP- versus hAAT-treated Gaa−/− mice. Conversely, GAA activity achieved with LiMP in Gaa−/− heart (Figure 6C), diaphragm (Figure 6D), triceps (Figure 6E), and quadriceps (Figure S9G) was significantly higher compared with hAAT, highlighting its efficient dual transcriptional activity. Consistently, significantly higher amounts of sec-hGAA protein were detected in triceps (as representative muscle; Figures S9H and S9I). AAV9-LiMP also provided significantly higher enzyme levels to the spinal cord compared with hAAT (Figure 6F; Figure S10A), likely mediated by the higher levels of *GAA* transgene expression achieved with LiMP in muscle. Accordingly, transgene mRNA expression in the spinal cord showed no significant differences in transcriptional activity of LiMP and hAAT promoters (Figure S10B). Conversely, both LiMP and the hAAT promoter showed significantly lower activity compared with LiNeuP (Figures S10B–S10D).

Slightly higher brain GAA protein levels were observed when using LiMP versus the hAAT promoter (Figure 6G; Figure S10E), although the differences were not statistically significant. As observed in the high-dose study (Figures S8E and S8F), GAA activity in the CNS was not significantly different from untreated Gaa−/− mice (Ctrl; Figures S10F and S10G) because of the low sensitivity of the assay used.

Pathological glycogen accumulation was significantly reduced upon treatment with LiMP vectors in heart (Figure 6H), diaphragm (Figure 6I), quadriceps (Figure S10H), and triceps (Figure 6J) of Gaa−/− mice compared with both untreated (Ctrl) and hAAT-treated Gaa−/− mice. In spinal cord and brain, a significant glycogen reduction was observed in all AAV-treated Gaa−/− mice compared with untreated Gaa−/− mice (Ctrl), although at levels still different from unaffected Gaa+/+ (Figure 6K). Because hGAA-mediated glycogen clearance in the CNS improves over time,[47] the higher amounts of enzyme provided by LiMP compared to the hAAT promoter (Figures 6F and 6G; Figures S10A–S10E) could result in improved therapeutic efficacy upon extended follow-up. Significant rescue of cardiomegaly (Figure 7A) and muscle strength (Figure 7B) was observed only in Gaa−/− mice treated with LiMP vectors. VGCNs in the liver (Figure S11A) and quadriceps (Figure S11B) showed similar levels of tissue transduction.

No IgG to sec-hGAA was detected in the plasma of AAV-treated Gaa−/− mice analyzed monthly by ELISA, confirming the prevention of anti-hGAA immunity (Table S2). IgGs to the vector capsid were instead observed in AAV9-treated mice (Table S2).

We next asked whether systemic AAV gene delivery of *sec-hGAA* using LiNeuP expressing in liver and CNS could rescue muscle strength

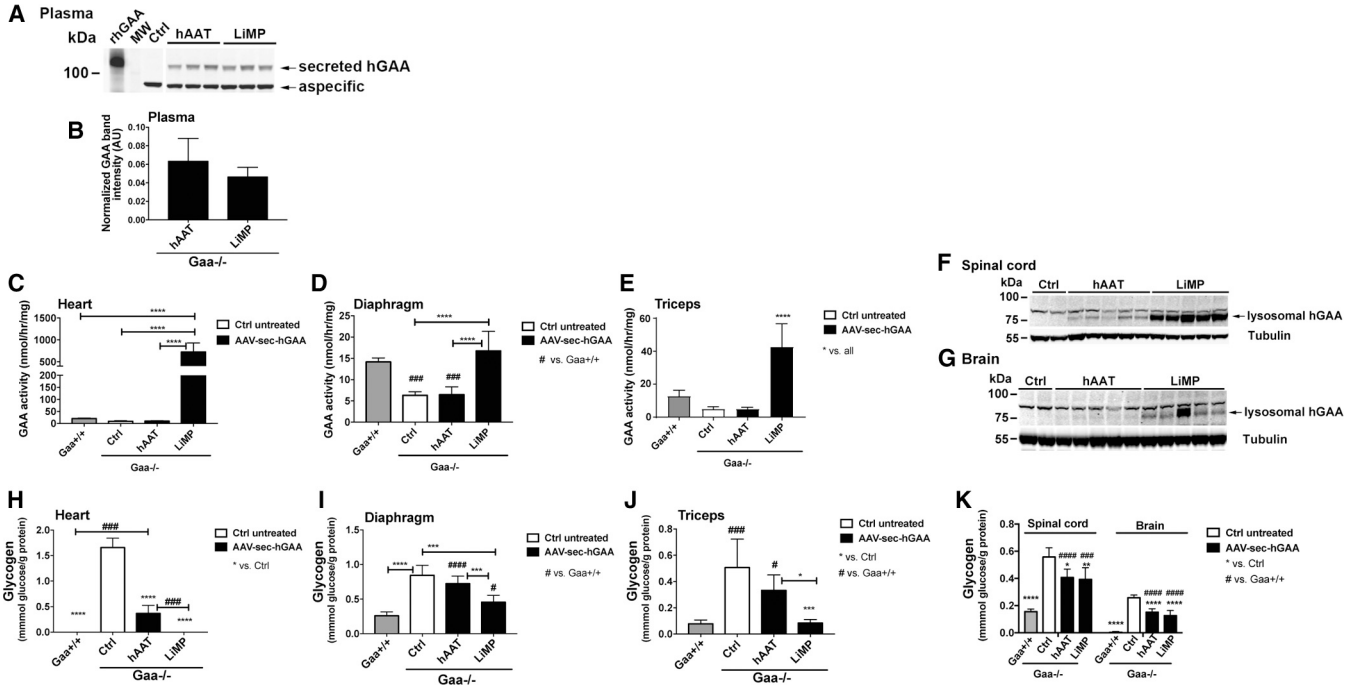

Figure 6. Rescue of the Disease Phenotype of Gaa–/– Mice Treated as Neonates with Low-Dose AAV Gene Therapy Using LiMP

(A–K) Analysis of hGAA transgene expression (A–G) and rescue of disease phenotype (H–K) in 4-month-old Gaa−/− mice treated as neonates with intravenous injection of AAV9 vectors (dose, 6×10^{12} vg/kg) encoding a codon-optimized sec-hGAA under the control of LiMP (n = 5) or hepatocyte-specific (hAAT, n = 5) promoter for comparison. Untreated Gaa−/− mice were used as affected controls (n = 5); littermate Gaa+/+ mice were used as unaffected controls (n = 6). (A) Representative western blot of Gaa−/− plasma with anti-human GAA antibody. The molecular weight marker (kilodaltons) is depicted. rhGAA was loaded as a positive control. (B) Quantification of hGAA protein band in Gaa−/− plasma normalized by the aspecific band. (C–E) Analysis of GAA enzyme activity in muscles: heart (C), diaphragm (D), triceps (E). (F and G) Western blot analyses of Gaa−/− spinal cord (F) and brain (G) with anti-human GAA antibody; anti-tubulin antibody was used as a loading control. The molecular weight marker (kilodaltons) is depicted. The western blot quantification is shown in Figures S10A and S10E. (H–K) Glycogen accumulation measured in muscle (H–J) and the CNS (K). Data are depicted as average ± SD; n = 5–6 mice per cohort as described above. Statistical analysis: Student's t test (B), one-way ANOVA with Tukey *post hoc* (C–E and H–K). *p < 0.05, **p < 0.01, ***p < 0.001, ****p < 0.0001, #p < 0.05, ###p < 0.001. Asterisks and hash marks on the bars show significant differences versus mouse cohorts specified in the legends.

similarly as LiMP. Interestingly, treatment of neonate Gaa−/− mice with AAV9-LiNeuP-*sec-hGAA* vectors at the same vector doses resulted in no significant improvement of grip test muscle strength compared with untreated Gaa−/− mice 4 months after treatment (Gaa−/− LiNeuP [n = 5], 1.65 ± 0.06; Gaa−/− Ctrl, 1.4 ± 0.05; one-way ANOVA with Tukey *post hoc* p = 0.5). This observation confirms the importance of simultaneous expression of GAA in liver and muscle for the long-term rescue of PD in neonate mice. The transcriptional activity of LiMP in muscle was further confirmed in human myoblasts *in vitro* (Figure S12).

Overall, these results show that LiMP prevents anti-GAA immunity and achieves superior therapeutic efficacy in neonate animals following systemic AAV liver gene therapy at low vector doses.

DISCUSSION

Gene therapy relies on the ability to achieve long-term transgene expression at therapeutic levels with a single intervention. Here we report the development of a novel tandem promoter design promoting hepatic tolerance while driving efficient and persistent extra-hepatic transgene expression. We applied our technology to infantile PD,[37] a severe neuromuscular disorder characterized by early onset, systemic manifestations, and high immunogenicity of the missing enzyme.

We showed that combination of the liver-specific enhancer-promoter ApoE-hAAT with either the muscle promoter spC5.12 or the neuronal promoter hSYN resulted in the generation of efficient tandem liver-muscle and liver-neuron promoters (LiMP and LiNeuP, respectively). In the context of systemic AAV gene delivery for PD, the use of LiMP and LiNeuP resulted in specific *hGAA* transgene co-transcription in liver in addition to muscle and CNS, respectively, and hepatically mediated prevention of anti-hGAA immunity in immunocompetent Gaa−/− mice. This finding is particularly relevant for gene delivery to muscle, a tissue reported to be highly pro-immunogenic.[9,26,32,36,76,77]

Immunity to GAA is an important limitation in the treatment of PD because formation of neutralizing antibodies can be associated with a poor prognosis in patients with the infantile form of the disease treated with ERT.[39,42,43] Previous gene transfer studies have shown

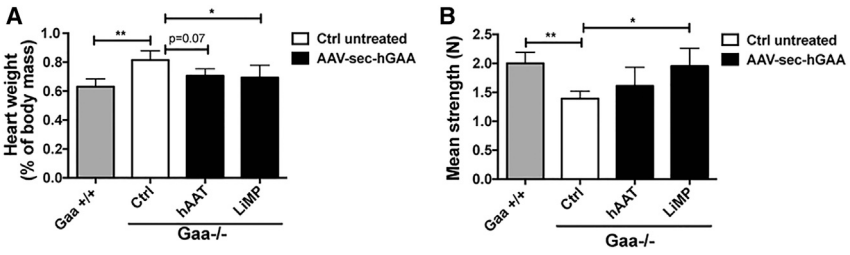

Figure 7. Rescue of Cardiomegaly and Muscle Strength in Gaa–/– Mice Treated as Neonates with Low-Dose AAV Gene Therapy Using LiMP

(A and B) Rescue of the disease phenotype in 4-month-old Gaa−/− mice treated as neonates with intravenous injection of AAV9 vectors (dose, 6×10^{12} vg/kg) encoding a codon-optimized sec-hGAA under the control of LiMP (n = 5) or hepatocyte-specific hAAT promoter (n = 5) for comparison. Untreated Gaa−/− mice were used as affected controls (n = 5); littermate Gaa+/+ mice were used as unaffected controls (n = 6). (A) Heart weight normalized by body weight. (B) Muscle strength measured by 4-limb grip test. (A and B) Data are depicted as average ± SD; n = 5–6 mice per cohort as described above. Statistical analysis: one-way ANOVA with Tukey *post hoc*. *$p < 0.05$, **$p < 0.01$.

that hepatocyte-restricted expression prevents transgene immune responses in PD[7,47,68] and other diseases.[11,12] Here we show that AAV-*hGAA* gene therapy using LiMP also results in avoidance of anti-transgene immune responses together with a significant decrease in established anti-hGAA immunity triggered by previous ERT treatment.

Previous work explored the use of two separate transgene expression cassettes, one active in hepatocytes and the other in muscle, packaged in a mixture of AAV vectors, to treat Gaa−/− mice.[78] Although this approach showed therapeutic efficacy and induction of hepatic tolerance to the GAA transgene product, it carries significant drawbacks, including the need for manufacturing two separate AAV vectors and delivery of inactive transgene expression cassettes to both hepatocytes and muscle (hepatocyte-specific promoters are not active in muscle, and, vice versa, muscle-specific promoters are not active in liver). In contrast, the tandem monocistronic transgene expression cassette described here has the advantage of being packaged in a single AAV vector and being simultaneously transcriptionally active in all desired target tissues. This is associated with persistent therapeutic efficacy in neonate animals and consistent prevention of the anti-hGAA humoral immune response at vector doses of up to 25 times lower than what has been reported previously.[78] Furthermore, our strategy could be applied to other diseases in which anti-transgene immune responses are a concern. One example of such diseases are muscular dystrophies,[5] in which detrimental anti-transgene immune responses are triggered by pathological muscle damage that creates a pro-inflammatory environment.[9,26,27,31,36,76,77]

AAV gene transfer to the CNS has also been reported to induce anti-transgene immune responses that prevent therapeutic efficacy in animal models of CNS diseases.[33,34,71] This has prompted the use of immunosuppressive regimens in human clinical trials to prevent anti-transgene immunity.[21–23] Accordingly, the use LiNeuP may help address this issue by avoiding detrimental transgene immunity in nervous tissue via liver-mediated tolerance induction.

AAV vector genomes persist in the host cell nuclei mostly as episomes.[13–15,17] Consequently, one important limitation of liver gene therapy with AAV vectors in pediatric diseases such as infantile PD is transgene persistence.

Our data indicate that systemic AAV gene therapy with the tandem LiMP promoter in neonate Gaa−/− mice provided superior and persistent therapeutic efficacy compared with single tissue-specific promoters. Complete clearance of whole-body pathological glycogen accumulation and significant rescue of cardiac hypertrophy and muscle strength were indeed measured only when using LiMP. As expected,[14–17] partial loss of liver expression because of hepatocyte proliferation was observed in neonate animals treated with the LiMP vector. However, this was not associated with lack of therapeutic efficacy because of the persistence of transgene expression in muscle driven by the dual tissue specificity of the promoter. Previous studies of AAV gene therapy in neonate Gaa−/− mice showed only partial rescue of the disease phenotype.[30,79] One study showed glycogen reduction in the CNS with no muscle rescue upon intracerebroventricular (i.c.v.) administration of AAV vectors expressing *GAA* under the control of the hSYN neuron-specific promoter.[79] These findings are consistent with the lack of rescue of muscle strength we observed in neonate Gaa−/− mice treated with LiNeuP. In another study, neonate Gaa−/− mice treated with intravenous delivery of AAV1-CMV-GAA presented a glycogen reduction in the heart and diaphragm.[30] However, CMV-driven *GAA* expression resulted in development of persistent high-titer anti-hGAA IgG.[30] Similarly, immunosuppression was required to prevent anti-GAA humoral immune responses in infantile PD patients receiving an AAV1-CMV-GAA vector via intra-diaphragmatic delivery.[20]

One interesting aspect of the tandem promoter LiMP is the ability to drive high muscle expression superior to that of the muscle-specific C5.12 promoter, suggesting a synergy among the different transcription regulatory elements. Notably, LiMP-mediated expression of secretable hGAA in muscle also resulted in superior enzyme targeting to the CNS compared with both the C5.12 and hAAT promoters. This may possibly result from facilitated protein trafficking between muscle fibers and neurons (e.g., at the neuromuscular junction level), which would overcome the restrictions posed by the blood-brain barrier.[80,81]

Combined with the expression of secretable hGAA, the LiMP-based approach, but not the single promoter approach, significantly rescued the muscle strength of Gaa−/− mice treated at birth with low vector doses (3×10^{13} vg/kg to 6×10^{12} vg/kg), which are ~10–50 times lower

than those currently used in other studies of neonatal AAV gene therapy.[16,82–86] This is an important goal in the treatment of lethal neuromuscular diseases, in which the high vector doses required[19,27,77] pose safety concerns[58,87] and manufacturing challenges.[88]

Previous reports have shown the activity of the selected single transcriptional regulatory elements in large animal models and human cells;[48,50,53] this is consistent with the observed activity of the LiMP in human hepatocyte and myoblasts. However, one limitation of the current work is the lack of studies in large animal models aimed at defining transgene persistence in neonate animals and therapeutic vector doses. Future work will have to address this point, particularly given the generally reduced transduction efficiency of AAV vectors in non-human primates (NHPs) compared with mice.[89] Of note, recent studies in fetal rhesus monkeys treated with AAV vectors showed persistent expression in muscle but not liver,[17] supporting the overall model of persistent therapeutic expression mediated by LiMP presented here. In our study, therapeutic efficacy in neonate mice was observed with AAV serotypes currently in the clinic for the treatment of pediatric neuromuscular disorders (Clinicaltrials.gov: NCT02122952 and NCT03199469),[19,27] but other naturally occurring or engineered AAVs with a similar transduction pattern could be tested. Given that high AAV vector doses ($>10^{14}$ vg/kg) are required to transduce skeletal muscle and nervous tissue in large animal models[24,50] and humans,[19,27] application of the tandem promoter approach described here is primarily restricted to infantile PD and other congenital conditions in which the persistence of transgene expression in the liver is a hurdle for long-term efficacy. For adults with late-onset PD[90] or other protein deficiencies rescued by liver-directed gene transfer, the use of an hepatocyte-restricted promoter still remains the most efficient approach, as demonstrated in animal models[47,60,61] and clinical trials.[49,91]

Finally, another possible limitation of the approach presented here is related to the size of the regulatory elements used, considering the maximum efficient packaging capacity of AAV vectors (~5 kb). Although this is not a limitation for PD and other diseases caused by mutations in genes with a short coding sequence (up to ~3 kb),[19,21–23,33,34,47] the generation of smaller tandem promoters or the use of dual AAV vectors[59,92] will help address this point.

In conclusion, here we describe a novel gene therapy strategy based on the use of tandem promoter monocistronic expression cassettes packaged into a single AAV vector. This approach allows concomitant liver-mediated prevention of anti-transgene immunity and persistent expression in non-hepatic tissues in neonate mice. This work addresses important limitations of AAV-mediated gene transfer for the treatment of systemic, multi-organ conditions characterized by transgene immunogenicity and requiring therapeutic intervention early in life.

MATERIALS AND METHODS

Experimental Design

The objective of this study was to evaluate the transcriptional activity, immunogenicity, and therapeutic efficacy of our newly generated tandem promoters in the context of systemic AAV gene therapy. To evaluate the promoter transcriptional activity, we performed experiments *in vitro* and *in vivo*. For the *in vitro* experiments, we used commercially available cell lines. The number of sampled units, n, was considered a single independent experiment (n = 1); for all *in vitro* experiments, $n \geq 2$. Readouts of the *in vitro* studies were hGAA protein expression and GAA enzyme activity. For the *in vivo* studies, we generated and used two serotypes, AAV8 and AAV9, based on their efficient transduction of liver, muscle, and nervous system.[24,50,63–65,73,75,93] To evaluate the activity of the tandem promoters in tissues *in vivo*, we used wild-type male C56BL/6 mice treated with intravenous injection of AAV vectors containing the transgene of interest under the control of the tested promoters. To evaluate the immunogenicity and therapeutic efficacy of gene transfer using the tandem promoter, we used a mouse model of PD treated with intravenous injection of AAV vectors containing therapeutic *hGAA* transgenes under the control of the tested promoters. Littermate male mice were used, either affected (Gaa−/−) or healthy (Gaa+/+). Because neonate mice are more prone to tolerance,[69–71] adult Gaa−/− mice were specifically treated with AAV to properly evaluate anti-transgene immune responses. For the *in vivo* studies, we used two *hGAA* transgenes that have been described previously:[47] the native codon-optimized human GAA transgene (hGAA) and a modified version of the hGAA transgene encoding for a secretable enzyme form (sec-hGAA). The transgene encoding for the native hGAA enzyme (hGAA) was specifically used to evaluate humoral immune responses and promoter activity in adult mice; the transgene encoding for the secretable hGAA enzyme (sec-hGAA) was specifically used to evaluate the therapeutic efficacy of the tandem promoter approach in Gaa−/− mice treated as neonates because we have shown previously that sec-hGAA has a lower immunogenicity and superior therapeutic efficacy than the native hGAA form.[47] Readouts of the *in vivo* studies were *hGAA* mRNA expression in tissues to evaluate promoter transcriptional activity, anti-hGAA IgG levels to evaluate the humoral immune response upon AAV-*hGAA* gene transfer, hGAA protein expression, GAA enzyme activity, tissue glycogen content, heart weight, and muscle strength analyses to evaluate the therapeutic efficacy of AAV-*hGAA* gene therapy. For the *in vivo* experiments in mice, the number of sampled units, n, was considered a single mouse (n = 1); the number of mice per cohort is indicated in the figure legends. Mice were assigned randomly to the experimental groups.

Generation of GAA Expression Cassettes

The *GAA* transgene expression cassettes used in this study contained a codon-optimized version of the hGAA coding sequence we reported previously.[47] Codon optimization was performed using a commercial algorithm (Thermo Fisher Scientific).[47] The *hGAA* transgenes used in this study were *hGAA*, encoding the full-length hGAA protein, or *sec-hGAA*, encoding an engineered secretable GAA having an heterologous signal peptide and a deletion of 8 amino acids in the propeptide (reported in our previous study as sp7-Δ8-hGAAco[47] and abbreviated sec-hGAA in the present manuscript). We previously described the generation and properties of hGAA and sec-hGAA.[47] The *hGAA* and *sec-hGAA* transgenes were cloned in *cis* plasmids for AAV vector

production under the transcriptional control of the various tested promoters. The control promoters were the hepatocyte-specific hAAT promoter composed of the ApoE enhancer and the hAAT promoter,[94] the muscle-specific synthetic promoter C5.12 (spC5.12, abbreviated as C5.12),[50,55,56] the neuron-specific hSYN promoter,[51] the ubiquitous CAG promoter composed of the CMV early enhancer and the chicken β-actin (CBA) promoter (abbreviated as CAG), and the newly generated tandem promoters (Enh.C5.12, LiMP, and LiNeuP) depicted in Figure 1A. The expression cassettes contained an intron between the promoter and the transgene start codon and a polyadenylation signal after the transgene stop codon and were flanked by the ITRs of AAV2. All DNA sequences used in this study were synthetized either by GeneCust or Thermo Fisher Scientific and are available upon request.

The full nucleotide sequences of all the transcription regulatory elements used are reported in the Supplemental Materials and Methods.

Studies in Cell Lines

Human hepatoma cells (HuH7, Thermo Fisher Scientific),[47] mouse myoblast cells (C2, ATCC CRL-1772), and mouse neuronal cells (NSC34, Cedarlane)[62] were seeded in 6-well plates (5×10^5 cells/well) and transfected with plasmids encoding *sec-hGAA* (2 μg/well) using Lipofectamine 3000 in OPTIMEM medium (Thermo Fisher Scientific) according to the manufacturer's instructions. A plasmid encoding EGFP under the control of the phosphoglycerate kinase (PGK) promoter (2 μg/well) was transfected as a control. 200 ng/well of the PGK-*EGFP* plasmid were co-transfected with *sec-hGAA* plasmids to normalize transfection efficiency. 72 hr after transfection, cells and conditioned media were harvested and analyzed for GAA enzyme activity and hGAA expression by western blot analyses. Early-passage cell cultures were used in the study.

Human skeletal muscle myoblasts (CSC-C3196, Creative Bioarray) were seeded on collagen-coated 12-well plates and infected with AAV9-*hGAA* or AAV9-EGFP vectors for 2 hr in OPTIMEM medium (Thermo Fisher Scientific) at an MOI of 2×10^5 vg/cell. After infection, cells were maintained using the Creative Bioarray SuperCult Skeletal Muscle Cell Growth Medium Kit supplemented with 10% fetal bovine serum and human fibroblast growth factor-2 (FGF-2, Miltenyi Biotec). Infection was repeated twice, every 48 hr; cells were harvested 48 hr following the second infection.

AAV Vector Production

The AAV vectors used in this study were produced using an adenovirus-free transient transfection method of HEK293 cells and purified by CsCl gradient as described previously.[94] Titers of AAV vector stocks were determined using real-time qPCR and SDS-PAGE, followed by SYPRO Ruby protein gel stain and band densitometry. All vector preparations used in the study were titered side by side before use. The primers used for qPCR on the AAV genome annealed to codon-optimized *hGAA* transgene sequence: forward: 5′-agatacgccggacattggactg-3′; reverse, 5′-agatacgccggacattggactg-3′. The AAV serotypes used were either AAV8 or AAV9, which have a similar transduction profile upon systemic administration to mice[24,50,63–65,73,75,93,94] and are currently tested in the clinic for the treatment of pediatric neuromuscular disorders.[19,27]

In Vivo Studies

Mouse studies were performed according to the French and European legislation regarding animal care and experimentation (2010/63/EU) and approved by the local institutional ethical committee (protocols 2015-008, 2016-019, and 2016052412533889). Wild-type male C57BL/6 mice were purchased from Charles River Laboratories. Gaa knockout mice (Gaa−/−) were purchased from The Jackson Laboratory (B6;129-Gaatm1Rabn/J, stock number 004154, 6neo) and were originally generated by Raben et al.[95] Littermate male mice were used, either affected (Gaa−/−) or healthy (Gaa+/+). We have reported the phenotype of male Gaa−/− versus Gaa+/+ mice from our colony in previous work.[47]

AAV vectors were delivered to adult mice via the tail vein in a volume of 0.2 mL and neonate mice on post-natal days 1 and 2 via the temporal vein in a volume of 0.03 mL. Mouse experimental groups were sized at $n \geq 4$ based on data generated in a previous study;[47] all samples and animals analyzed were included in the data, and none of the outliers were excluded. The only exception is shown in Figure 2D, the C5.12 group, in which one mouse was removed from the analyses because of bad mRNA quality (n = 3 of 4). For the gene expression analyses, C57BL/6 (n = 4/group; Figure 2) or Gaa−/− mice (n = 3/group; Figures S3B–S3E) were treated with 2×10^{12} vg/kg of AAV9 vector injected intravenously. To evaluate the immunogenicity of tandem promoters, we performed three independent mouse studies. In the first study, Gaa−/− mice (n = 5/group) were treated with 2×10^{12} vg/kg of AAV9 vector injected intravenously. In the second study, Gaa−/− mice (n = 4–5 per group) were treated with 2×10^{12} vg/kg of AAV8 vector injected intravenously. In the third study, we evaluated the eradication of pre-existing anti-hGAA IgG in Gaa−/− mice. To this aim, 14 mice were treated with intravenous injection of rhGAA at a dose of 20 mg/ kg[68] every 2 weeks for a total of 3 administrations. Each rhGAA infusion was performed 15 min after intraperitoneal administration of 25 mg/kg of antihistaminic (diphenhydramine hydrochloride), as described previously.[68] Two weeks after the last rhGAA administration, anti-hGAA IgG were measured. The immunized Gaa−/− mice (n = 8) were assigned to three AAV9 treatment groups (2×10^{12} vg/kg; AAV-Ctrl, n = 2; AAV-hAAT, n = 3; AAV-LiMP n = 3). For studies of therapeutic efficacy in the Pompe mouse model, neonate mice were assigned to the unaffected (Gaa+/+, n = 8–6) or affected cohort (Gaa−/−). Affected Gaa−/− mice were randomly assigned to the control group (Ctrl, untreated Gaa−/−, n = 5-–6/cohort) or to the different AAV treatment groups (n = 5–6/cohort). To evaluate the therapeutic efficacy of AAV gene therapy in Pompe mice treated as neonates using our newly generated tandem promoters, we performed two independent mouse studies using either AAV8 (dose, 3×10^{13} vg/kg) or AAV9 (dose, 6×10^{12} vg/kg). For the *in vivo* studies, the operators who performed vector delivery, sample and tissue collection, and functional analyses (grip test) were blinded to the treatment groups.

GAA Activity Assay

Snap-frozen tissues were homogenized in UltraPure DNase- and RNase-free distilled water (Thermo Fisher Scientific). Tissues were weighed, homogenized, and centrifuged for 20 min at 10,000 × *g* to collect the supernatant. The enzymatic reaction was set up using 10 μL of sample (plasma or tissue homogenate) diluted appropriately and 20 μL of substrate, 4-methylumbelliferone (4MU)α-D-glucoside, in black 96-well plates (PerkinElmer). The reaction mixture was incubated at 37°C for 1 hr and then stopped by adding 150 μL of sodium carbonate buffer (pH 10.5). A standard curve (0–2,500 pmol/μL of 4MU) was used to measure released fluorescent 4MU from the individual reaction mixture using the EnSpire Alpha plate reader (PerkinElmer) at 449 nm (emission) and 360 nm (excitation). The protein concentration of the clarified supernatant was quantified by BCA (Thermo Fisher Scientific). To calculate the GAA activity in tissues, the released 4MU concentration was divided by the sample protein concentration, and activity was reported as nanomoles per hour per milligram protein.

Measurement of Glycogen Content

Homogenates of mouse tissues were prepared as indicated for GAA activity. Glycogen content was measured indirectly in tissue homogenates as glucose released after total digestion with *Aspergillus niger* amyloglucosidase (Sigma-Aldrich), as reported previously.[47] Samples were incubated for 5 min at 95°C and then cooled at 4°C; 25 μL of amyloglucosidase diluted 1:50 in 0.1 M potassium acetate (pH 5.5) was then added to each sample. A control reaction without amyloglucosidase was prepared for each sample. Both digestion and control samples were incubated at 37°C for 90 min and then at 95°C for 5 min. The glucose released was determined using a colorimetric assay (glucose assay kit, Sigma-Aldrich) and by measuring the absorbance at 540 nm using an EnSpire Alpha plate reader (PerkinElmer).

Vector Genome Copy Number Analysis

DNA was extracted from tissues homogenates using Nucleospin 8 (Macherey-Nagel, France) and quantified. Vector genome copy number was determined by qPCR using 100 ng of DNA, primers, and a probe annealed on the codon-optimized hGAA (forward, 5′-agatacgccggacattggactg-3′; reverse, 5′-agatacgccggacattggactg-3′; probe, 5′-gtgtggtcctcttgggagc-3′). Either the Sybergreen or TaqMan method was used as described previously.[47] VGCNs were normalized by microgram of DNA used in the qPCR. To quantify VGCN per diploid genome, DNA was extracted from tissue homogenates using the Gentra Puregene Tissue Kit (QIAGEN) and quantified. VGCN was determined by qPCR using 100 ng of DNA, primers, and a probe annealed on the codon-optimized hGAA transgene sequence (forward: 5′-agatacgccggacattggactg-3′; reverse: 5′-agatacgccggacattggactg-3′; probe, 5′-gtgtggtcctcttgggagc-3′) and mouse *Titin* as a reference gene (forward: 5′-aaaacgagcagtgacgtgagc-3′; reverse: 5′-ttcagtcatgctgctagcgc-3′; probe, 5′-tgcacggaagcgtctcgtctcagt-3′). The qPCR was performed using the TaqMan method, as described previously.[47,94]

RNA Extraction and Expression Analysis

Snap-frozen tissues were homogenized in Trizol reagent (Thermo Fisher Scientific). Total RNA was extracted from tissue homogenates using the PureLink RNA mini kit with the PureLink DNase set (Thermo Fisher Scientific). RNA was quantified, and 2–5 μg was retro-transcribed to cDNA using the Maxima First Strand cDNA Synthesis Kit for qRT-PCR with dsDNase (Thermo Scientific); RT-minus reactions were performed as a negative control. For *hGAA* mRNA expression analyses, the qPCR on cDNA was performed using Sybergreen and primers annealing specifically on the codon-optimized *hGAA* transgene sequence (hGAA forward, 5′-agatacgccggacattggactg-3′; hGAA reverse, 5′-agatacgccggacattggactg-3′). Primers annealing on the mouse *Actin* gene were used to normalize *hGAA* expression (*Actin* forward, 5′-ggctgtattcccctccatcg-3′; *Actin* reverse, 5′-ccagttggtaacaatgccatgt-3′) for the data depicted in Figure 2. Mouse *Actin* and *beta-2 microglobulin* (*B2m*; *B2m* forward, 5′-ggtctttctggtgcttgtctca-3′; *B2m* reverse, 5′-gttcggcttcccattctcc-3′) were used to normalize *hGAA* expression for the data depicted in Figures S3B, S3C, and S10B.

Western Blot Analysis

HuH7, C2, and NSC34 cell lysates were prepared using 10 mM PBS (pH 7.4) containing 1% of Triton X-100 and protease inhibitors (Roche Diagnostics). Western blot on mouse plasma was performed on samples diluted 1:4 in distilled water. Homogenates of mouse tissues were prepared as indicated for GAA activity. Protein concentration was determined using the BCA protein assay (Thermo Fisher Scientific). SDS-PAGE electrophoresis was performed in a 4%–12% polyacrylamide gel. After transfer, the membrane was blocked with Odyssey buffer (LI-COR Biosciences) and incubated with an anti-GAA antibody (rabbit monoclonal, clone EPR4716(2), Abcam), anti-EGFP (mouse monoclonal, sc-9996, Santa Cruz Biotechnology), anti-tubulin (mouse monoclonal, clone DM1A, Sigma-Aldrich), or anti-Gapdh (rabbit polyclonal, PA1-988, Thermo Fisher Scientific). The membrane was washed and incubated with the appropriate secondary antibody (LI-COR Biosciences) and visualized with the Odyssey imaging system (LI-COR Biosciences). For western blot quantification, we used either ImageJ or Image Studio Lite 4.0. The quantification of the hGAA protein bands in mouse tissues was normalized using either tubulin or Gapdh bands. The quantification of the hGAA protein band in plasma was normalized using a non-specific band detected by the anti-hGAA antibody in mouse plasma (used as a loading control).

Anti-GAA and Anti-capsid Antibody Detection

Anti-hGAA and anti-AAV capsid IgG capture assays were performed as described previously.[47] Briefly, Maxisorp 96-well plates (Thermo Fisher Scientific) were coated with 2 μg/mL of rhGAA or 2×10^{10} vector particles/mL (50 μL/well, AAV8 or AAV9). IgG standard curves were made by serial 1 to 2 dilution of commercial mouse recombinant IgGs (Sigma-Aldrich) that were coated directly onto the wells in duplicate (from 1 μg/mL to 0.15 μg/mL). Plasma samples appropriately diluted in 10 mM PBS (pH 7.4) containing 2% BSA were analyzed in duplicate. An HRP-conjugated anti-mouse IgG antibody (human ads-HRP, Southern Biotech) was used as a secondary antibody. Plates were revealed with OPD substrate (o-phenylenediaminedihydrochloride, Sigma). The reaction was stopped with H_2SO_4

3 M solution, and optical density (OD) measurements were done at 492 nm using a microplate reader (ENSPIRE, PerkinElmer, Waltham, USA). Anti-AAV IgG concentration was determined against the standard curve.

Immunofluorescence for hGAA on Liver Histological Sections

For liver histology, after mouse euthanasia, one lobe of the liver was snap-frozen in isopentane (−160°C) previously chilled in liquid nitrogen. Serial 12-μm cross-sections were cut in a Leica CM3050 S cryostat (Leica Biosystems). Two to four mice representative of the tested cohort were randomly selected. Liver sections were fixed with 4% paraformaldehyde (PFA), blocked and permeabilized with 10% normal goat serum (NGS) in 0.1% Triton X-100 for 3 hr at room temperature and stained with the primary anti-hGAA antibody (rabbit monoclonal, clone EPR4716(2), Abcam) overnight at 4°C. After washing, the sections were incubated with anti-rabbit Alexa Fluor 488 (Thermo Fisher Scientific) combined with DAPI. Representative images were acquired with an SP8 confocal microscope (Leica).

Grip Test

Grip strength was measured using a grip strength meter (Bioseb Grip Test 25N) as reported previously.[47] Briefly, three independent measurements of the strength of the four limbs were averaged. Mean values of grip strength are reported. The operator performing the grip test was blinded to mouse treatment.

Statistical Analysis

All data shown in the present manuscript are reported as mean ± SD. The number of sampled units, n, upon which we reported statistics, is the single mouse for the *in vivo* experiments (one mouse is n = 1) and the single independent experiment for the *in vitro* studies using cell lines (one independent experiments, n = 1). GraphPad Prism 7.0 software was used for statistical analyses. We assessed the normal distribution of the data obtained from the different measurements (mRNA expression in tissues, anti-hGAA IgG amounts in plasma, hGAA protein expression in plasma, cell lines and tissues, GAA enzyme activity in tissues, glycogen content in tissues, heart weight, and muscle functional analyses) using the Shapiro-Wilk test. The statistical tests used were unpaired Student's t test for two-group comparisons, one-way ANOVA with Tukey *post hoc* for comparisons of more than two groups, and two-way ANOVA with Tukey or Sidak *post hoc* for multiple variable comparisons. For all datasets analyzed by parametric tests, alpha = 0.05. All statistical tests were performed two-sided. $p < 0.05$ was considered significant. The statistical analysis performed for each dataset is indicated in the figure legends. For all figures, *$p < 0.05$, **$p < 0.01$, ***$p < 0.001$, ****$p < 0.0001$, #$p < 0.05$, ##$p < 0.01$, ###$p < 0.001$, ####$p < 0.0001$.

SUPPLEMENTAL INFORMATION

Supplemental Information includes Supplemental Materials and Methods, twelve figures, and two tables and can be found with this article online at https://doi.org/10.1016/j.omtm.2018.11.002.

AUTHOR CONTRIBUTIONS

P.C. and F.M. wrote the manuscript and conceived and directed the study. P.C. and P.S. performed data analysis and most of the experimental activity. H.C.-V., S.M., and S.C. contributed to the immunization studies. F.P. contributed to mouse study setup and biochemical analyses. M.S.-S., F.C., and S.C. produced the AAV vectors used in the studies. I.R. and C.L. contributed to transgene expression studies. L.v.W. performed the delivery of AAV vectors to mice and the harvesting of mouse samples. N.D. managed the organization of mouse studies. B.G. and S.M. contributed to liver histological studies. N.G. performed the grip test in mice.

CONFLICTS OF INTEREST

P.C., F.P., and F.M. are inventors of patent applications for the AAV treatment for Pompe disease licensed to Spark Therapeutics (WO2018046774 and WO2018046775). P.C. and F.M. are inventors of a patent application describing the use of tandem promoters. F.M. and F.C. are inventors of patents describing AAV-mediated liver gene transfer (CA2942451). F.M. is an employee of Spark Therapeutics.

ACKNOWLEDGMENTS

We thank Maria Grazia Biferi for kindly providing NSC34 cells and Evelyne Gicquel-Zouida for kindly providing human myoblast cells. This work was supported by Genethon and the French Muscular Dystrophy Association (A.F.M.). It was also supported by the European Union Research and Innovation Program under grant agreements 667751 (to F.M.) and 658712 (to F.M.), a European Research Council consolidator grant under grant agreement 617432 (to F.M.), and an ASTRE Laboratories of the Essonne General Council grant (to F.M.).

REFERENCES

1. Russell, S., Bennett, J., Wellman, J.A., Chung, D.C., Yu, Z.F., Tillman, A., Wittes, J., Pappas, J., Elci, O., McCague, S., et al. (2017). Efficacy and safety of voretigene neparvovec (AAV2-hRPE65v2) in patients with RPE65-mediated inherited retinal dystrophy: a randomised, controlled, open-label, phase 3 trial. Lancet *390*, 849–860.

2. Büning, H. (2013). Gene therapy enters the pharma market: the short story of a long journey. EMBO Mol. Med. *5*, 1–3.

3. LoDuca, P.A., Hoffman, B.E., and Herzog, R.W. (2009). Hepatic gene transfer as a means of tolerance induction to transgene products. Curr. Gene Ther. *9*, 104–114.

4. Herzog, R.W. (2017). Complexity of immune responses to AAV transgene products - Example of factor IX. Cell Immunol. Published online May 29, 2017. https://doi.org/10.1016/j.cellimm.2017.05.006.

5. Wang, Z., Tapscott, S.J., Chamberlain, J.S., and Storb, R. (2011). Immunity and AAV-Mediated Gene Therapy for Muscular Dystrophies in Large Animal Models and Human Trials. Front. Microbiol. *2*, 201.

6. Mingozzi, F., Liu, Y.L., Dobrzynski, E., Kaufhold, A., Liu, J.H., Wang, Y., Arruda, V.R., High, K.A., and Herzog, R.W. (2003). Induction of immune tolerance to coagulation factor IX antigen by in vivo hepatic gene transfer. J. Clin. Invest. *111*, 1347–1356.

7. Franco, L.M., Sun, B., Yang, X., Bird, A., Zhang, H., Schneider, A., Brown, T., Young, S.P., Clay, T.M., Amalfitano, A., et al. (2005). Evasion of immune responses to introduced human acid alpha-glucosidase by liver-restricted expression in glycogen storage disease type II. Mol. Ther. *12*, 876–884.

8. Lüth, S., Huber, S., Schramm, C., Buch, T., Zander, S., Stadelmann, C., Brück, W., Wraith, D.C., Herkel, J., and Lohse, A.W. (2008). Ectopic expression of neural

autoantigen in mouse liver suppresses experimental autoimmune neuroinflammation by inducing antigen-specific Tregs. J. Clin. Invest. *118*, 3403–3410.

9. Cao, O., Hoffman, B.E., Moghimi, B., Nayak, S., Cooper, M., Zhou, S., Ertl, H.C., High, K.A., and Herzog, R.W. (2009). Impact of the underlying mutation and the route of vector administration on immune responses to factor IX in gene therapy for hemophilia B. Mol. Ther. *17*, 1733–1742.

10. Nietupski, J.B., Hurlbut, G.D., Ziegler, R.J., Chu, Q., Hodges, B.L., Ashe, K.M., Bree, M., Cheng, S.H., Gregory, R.J., Marshall, J., and Scheule, R.K. (2011). Systemic administration of AAV8-α-galactosidase A induces humoral tolerance in nonhuman primates despite low hepatic expression. Mol. Ther. *19*, 1999–2011.

11. Finn, J.D., Ozelo, M.C., Sabatino, D.E., Franck, H.W., Merricks, E.P., Crudele, J.M., Zhou, S., Kazazian, H.H., Lillicrap, D., Nichols, T.C., and Arruda, V.R. (2010). Eradication of neutralizing antibodies to factor VIII in canine hemophilia A after liver gene therapy. Blood *116*, 5842–5848.

12. Markusic, D.M., Hoffman, B.E., Perrin, G.Q., Nayak, S., Wang, X., LoDuca, P.A., High, K.A., and Herzog, R.W. (2013). Effective gene therapy for haemophilic mice with pathogenic factor IX antibodies. EMBO Mol. Med. *5*, 1698–1709.

13. Nakai, H., Yant, S.R., Storm, T.A., Fuess, S., Meuse, L., and Kay, M.A. (2001). Extrachromosomal recombinant adeno-associated virus vector genomes are primarily responsible for stable liver transduction in vivo. J. Virol. *75*, 6969–6976.

14. Wang, L., Wang, H., Bell, P., McMenamin, D., and Wilson, J.M. (2012). Hepatic gene transfer in neonatal mice by adeno-associated virus serotype 8 vector. Hum. Gene Ther. *23*, 533–539.

15. Wang, L., Bell, P., Lin, J., Calcedo, R., Tarantal, A.F., and Wilson, J.M. (2011). AAV8-mediated hepatic gene transfer in infant rhesus monkeys (Macaca mulatta). Mol. Ther. *19*, 2012–2020.

16. Bortolussi, G., Zentillin, L., Vaníkova, J., Bockor, L., Bellarosa, C., Mancarella, A., Vianello, E., Tiribelli, C., Giacca, M., Vitek, L., and Muro, A.F. (2014). Life-long correction of hyperbilirubinemia with a neonatal liver-specific AAV-mediated gene transfer in a lethal mouse model of Crigler-Najjar Syndrome. Hum. Gene Ther. *25*, 844–855.

17. Conlon, T.J., Mah, C.S., Pacak, C.A., Rucker Henninger, M.B., Erger, K.E., Jorgensen, M.L., Lee, C.C., Tarantal, A.F., and Byrne, B.J. (2016). Transfer of Therapeutic Genes into Fetal Rhesus Monkeys Using Recombinant Adeno-Associated Type I Viral Vectors. Hum. Gene Ther. Clin. Dev. *27*, 152–159.

18. Coppoletta, J.M., and Wolbach, S.B. (1933). Body Length and Organ Weights of Infants and Children: A Study of the Body Length and Normal Weights of the More Important Vital Organs of the Body between Birth and Twelve Years of Age. Am. J. Pathol. *9*, 55–70.

19. Mendell, J.R., Al-Zaidy, S., Shell, R., Arnold, W.D., Rodino-Klapac, L.R., Prior, T.W., Lowes, L., Alfano, L., Berry, K., Church, K., et al. (2017). Single-Dose Gene-Replacement Therapy for Spinal Muscular Atrophy. N. Engl. J. Med. *377*, 1713–1722.

20. Corti, M., Liberati, C., Smith, B.K., Lawson, L.A., Tuna, I.S., Conlon, T.J., Coleman, K.E., Islam, S., Herzog, R.W., Fuller, D.D., et al. (2017). Safety of Intradiaphragmatic Delivery of Adeno-Associated Virus-Mediated Alpha-Glucosidase (rAAV1-CMV-hGAA) Gene Therapy in Children Affected by Pompe Disease. Hum. Gene Ther. Clin. Dev. *28*, 208–218.

21. Ellinwood, N.M., Ausseil, J., Desmaris, N., Bigou, S., Liu, S., Jens, J.K., Snella, E.M., Mohammed, E.E., Thomson, C.B., Raoul, S., et al. (2011). Safe, efficient, and reproducible gene therapy of the brain in the dog models of Sanfilippo and Hurler syndromes. Mol. Ther. *19*, 251–259.

22. Tardieu, M., Zérah, M., Gougeon, M.L., Ausseil, J., de Bournonville, S., Husson, B., Zafeiriou, D., Parenti, G., Bourget, P., Poirier, B., et al. (2017). Intracerebral gene therapy in children with mucopolysaccharidosis type IIIB syndrome: an uncontrolled phase 1/2 clinical trial. Lancet Neurol. *16*, 712–720.

23. Tardieu, M., Zérah, M., Husson, B., de Bournonville, S., Deiva, K., Adamsbaum, C., Vincent, F., Hocquemiller, M., Broissand, C., Furlan, V., et al. (2014). Intracerebral administration of adeno-associated viral vector serotype rh.10 carrying human SGSH and SUMF1 cDNAs in children with mucopolysaccharidosis type IIIA disease: results of a phase I/II trial. Hum. Gene Ther. *25*, 506–516.

24. Mack, D.L., Poulard, K., Goddard, M.A., Latournerie, V., Snyder, J.M., Grange, R.W., Elverman, M.R., Denard, J., Veron, P., Buscara, L., et al. (2017). Systemic AAV8-Mediated Gene Therapy Drives Whole-Body Correction of Myotubular Myopathy in Dogs. Mol. Ther. *25*, 839–854.

25. Falk, D.J., Soustek, M.S., Todd, A.G., Mah, C.S., Cloutier, D.A., Kelley, J.S., Clement, N., Fuller, D.D., and Byrne, B.J. (2015). Comparative impact of AAV and enzyme replacement therapy on respiratory and cardiac function in adult Pompe mice. Mol. Ther. Methods Clin. Dev. *2*, 15007.

26. Mendell, J.R., Campbell, K., Rodino-Klapac, L., Sahenk, Z., Shilling, C., Lewis, S., Bowles, D., Gray, S., Li, C., Galloway, G., et al. (2010). Dystrophin immunity in Duchenne's muscular dystrophy. N. Engl. J. Med. *363*, 1429–1437.

27. Kuntz, N., Shieh, P., Smith, B., Bönnemann, C., Dowling, J., and Lawlor, M. (2018). Aspiro Phase 1/2 Gene Therapy Trial in X-Linked Myotubular Myopathy (Xlmtm): Preliminary Safety and Efficacy Findings. The American Society of Gene and Cell Therapy (Chicago: ASGCT).

28. Sun, B., Zhang, H., Franco, L.M., Brown, T., Bird, A., Schneider, A., and Koeberl, D.D. (2005). Correction of glycogen storage disease type II by an adeno-associated virus vector containing a muscle-specific promoter. Mol. Ther. *11*, 889–898.

29. Sun, B., Young, S.P., Li, P., Di, C., Brown, T., Salva, M.Z., Li, S., Bird, A., Yan, Z., Auten, R., et al. (2008). Correction of multiple striated muscles in murine Pompe disease through adeno-associated virus-mediated gene therapy. Mol. Ther. *16*, 1366–1371.

30. Mah, C., Pacak, C.A., Cresawn, K.O., Deruisseau, L.R., Germain, S., Lewis, M.A., Cloutier, D.A., Fuller, D.D., and Byrne, B.J. (2007). Physiological correction of Pompe disease by systemic delivery of adeno-associated virus serotype 1 vectors. Mol. Ther. *15*, 501–507.

31. Fougerousse, F., Bartoli, M., Poupiot, J., Arandel, L., Durand, M., Guerchet, N., et al. (2007). Phenotypic Correction of alpha-Sarcoglycan Deficiency by Intra-arterial Injection of a Muscle-specific Serotype 1 rAAV Vector. Mol. Ther. *15*, 53–61.

32. Hoffman, B.E., Dobrzynski, E., Wang, L., Hirao, L., Mingozzi, F., Cao, O., and Herzog, R.W. (2007). Muscle as a target for supplementary factor IX gene transfer. Hum. Gene Ther. *18*, 603–613.

33. Hinderer, C., Bell, P., Gurda, B.L., Wang, Q., Louboutin, J.P., Zhu, Y., Bagel, J., O'Donnell, P., Sikora, T., Ruane, T., et al. (2014). Intrathecal gene therapy corrects CNS pathology in a feline model of mucopolysaccharidosis I. Mol. Ther. *22*, 2018–2027.

34. Passini, M.A., Bu, J., Fidler, J.A., Ziegler, R.J., Foley, J.W., Dodge, J.C., Yang, W.W., Clarke, J., Taksir, T.V., Griffiths, D.A., et al. (2007). Combination brain and systemic injections of AAV provide maximal functional and survival benefits in the Niemann-Pick mouse. Proc. Natl. Acad. Sci. USA *104*, 9505–9510.

35. Calcedo, R., Somanathan, S., Qin, Q., Betts, M.R., Rech, A.J., Vonderheide, R.H., Mueller, C., Flotte, T.R., and Wilson, J.M. (2017). Class I-restricted T-cell responses to a polymorphic peptide in a gene therapy clinical trial for α-1-antitrypsin deficiency. Proc. Natl. Acad. Sci. USA *114*, 1655–1659.

36. Boisgerault, F., and Mingozzi, F. (2015). The Skeletal Muscle Environment and Its Role in Immunity and Tolerance to AAV Vector-Mediated Gene Transfer. Curr. Gene Ther. *15*, 381–394.

37. van der Ploeg, A.T., and Reuser, A.J. (2008). Pompe's disease. Lancet *372*, 1342–1353.

38. Kishnani, P.S., and Beckemeyer, A.A. (2014). New therapeutic approaches for Pompe disease: enzyme replacement therapy and beyond. Pediatr. Endocrinol. Rev. *12* (*Suppl 1*), 114–124.

39. Kishnani, P.S., Goldenberg, P.C., DeArmey, S.L., Heller, J., Benjamin, D., Young, S., Bali, D., Smith, S.A., Li, J.S., Mandel, H., et al. (2010). Cross-reactive immunologic material status affects treatment outcomes in Pompe disease infants. Mol. Genet. Metab. *99*, 26–33.

40. de Vries, J.M., van der Beek, N.A., Kroos, M.A., Ozkan, L., van Doorn, P.A., Richards, S.M., Sung, C.C., Brugma, J.D., Zandbergen, A.A., van der Ploeg, A.T., and Reuser, A.J. (2010). High antibody titer in an adult with Pompe disease affects treatment with alglucosidase alfa. Mol. Genet. Metab. *101*, 338–345.

41. Banugaria, S.G., Prater, S.N., Patel, T.T., Dearmey, S.M., Milleson, C., Sheets, K.B., Bali, D.S., Rehder, C.W., Raiman, J.A., Wang, R.A., et al. (2013). Algorithm for the early diagnosis and treatment of patients with cross reactive immunologic material-negative classic infantile pompe disease: a step towards improving the efficacy of ERT. PLoS ONE *8*, e67052.

42. Kazi, Z.B., Desai, A.K., Berrier, K.L., Troxler, R.B., Wang, R.Y., Abdul-Rahman, O.A., Tanpaiboon, P., Mendelsohn, N.J., Herskovitz, E., Kronn, D., et al. (2017). Sustained immune tolerance induction in enzyme replacement therapy-treated CRIM-negative patients with infantile Pompe disease. JCI Insight *2*, 94328.

43. Poelman, E., Hoogeveen-Westerveld, M., Kroos-de Haan, M.A., van den Hout, J.M.P., Bronsema, K.J., van de Merbel, N.C., van der Ploeg, A.T., and Pijnappel, W.W.M.P. (2018). High Sustained Antibody Titers in Patients with Classic Infantile Pompe Disease Following Immunomodulation at Start of Enzyme Replacement Therapy. J. Pediatr. *195*, 236–243.e3.

44. Chien, Y.H., Hwu, W.L., and Lee, N.C. (2013). Pompe disease: early diagnosis and early treatment make a difference. Pediatr. Neonatol. *54*, 219–227.

45. Burton, B.K. (2012). Newborn screening for Pompe disease: an update, 2011. Am. J. Med. Genet. C. Semin. Med. Genet. *160C*, 8–12.

46. Zhang, P., Sun, B., Osada, T., Rodriguiz, R., Yang, X.Y., Luo, X., Kemper, A.R., Clay, T.M., and Koeberl, D.D. (2012). Immunodominant liver-specific expression suppresses transgene-directed immune responses in murine pompe disease. Hum. Gene Ther. *23*, 460–472.

47. Puzzo, F., Colella, P., Biferi, M.G., Bali, D., Paulk, N.K., Vidal, P., Collaud, F., Simon-Sola, M., Charles, S., Hardet, R., et al. (2017). Rescue of Pompe disease in mice by AAV-mediated liver delivery of secretable acid α-glucosidase. Sci. Transl. Med. *9*, eaam6375.

48. Manno, C.S., Pierce, G.F., Arruda, V.R., Glader, B., Ragni, M., Rasko, J.J., Ozelo, M.C., Hoots, K., Blatt, P., Konkle, B., et al. (2006). Successful transduction of liver in hemophilia by AAV-Factor IX and limitations imposed by the host immune response. Nat. Med. *12*, 342–347.

49. George, L.A., Sullivan, S.K., Giermasz, A., Rasko, J.E.J., Samelson-Jones, B.J., Ducore, J., Cuker, A., Sullivan, L.M., Majumdar, S., Teitel, J., et al. (2017). Hemophilia B Gene Therapy with a High-Specific-Activity Factor IX Variant. N. Engl. J. Med. *377*, 2215–2227.

50. Le Guiner, C., Servais, L., Montus, M., Larcher, T., Fraysse, B., Moullec, S., Allais, M., François, V., Dutilleul, M., Malerba, A., et al. (2017). Long-term microdystrophin gene therapy is effective in a canine model of Duchenne muscular dystrophy. Nat. Commun. *8*, 16105.

51. McLean, J.R., Smith, G.A., Rocha, E.M., Hayes, M.A., Beagan, J.A., Hallett, P.J., and Isacson, O. (2014). Widespread neuron-specific transgene expression in brain and spinal cord following synapsin promoter-driven AAV9 neonatal intracerebroventricular injection. Neurosci. Lett. *576*, 73–78.

52. Kügler, S., Kilic, E., and Bähr, M. (2003). Human synapsin 1 gene promoter confers highly neuron-specific long-term transgene expression from an adenoviral vector in the adult rat brain depending on the transduced area. Gene Ther. *10*, 337–347.

53. Wu, S.H., Liao, Z.X., D Rizak, J., Zheng, N., Zhang, L.H., Tang, H., He, X.B., Wu, Y., He, X.P., Yang, M.F., et al. (2017). Comparative study of the transfection efficiency of commonly used viral vectors in rhesus monkey (*Macaca mulatta*) brains. Zool. Res. *38*, 88–95.

54. Miao, C.H., Ohashi, K., Patijn, G.A., Meuse, L., Ye, X., Thompson, A.R., and Kay, M.A. (2000). Inclusion of the hepatic locus control region, an intron, and untranslated region increases and stabilizes hepatic factor IX gene expression in vivo but not in vitro. Mol. Ther. *1*, 522–532.

55. Li, X., Eastman, E.M., Schwartz, R.J., and Draghia-Akli, R. (1999). Synthetic muscle promoters: activities exceeding naturally occurring regulatory sequences. Nat. Biotechnol. *17*, 241–245.

56. Rasowo, B., Shilpita, S., Ermira, S., Marinee, C., and Vanden Driessche, T. (2014). Development of novel muscle-specific adeno-associated viral vector constructs for gene therapy of Duchenne muscular dystrophy. Eur. Sci. J. *10*.

57. Wu, Z., Yang, H., and Colosi, P. (2010). Effect of genome size on AAV vector packaging. Mol. Ther. *18*, 80–86.

58. Chandler, R.J., LaFave, M.C., Varshney, G.K., Trivedi, N.S., Carrillo-Carrasco, N., Senac, J.S., Wu, W., Hoffmann, V., Elkahloun, A.G., Burgess, S.M., and Venditti, C.P. (2015). Vector design influences hepatic genotoxicity after adeno-associated virus gene therapy. J. Clin. Invest. *125*, 870–880.

59. Vidal, P., Pagliarani, S., Colella, P., Costa Verdera, H., Jauze, L., Gjorgjieva, M., et al. (2018). Rescue of GSDIII Phenotype with Gene Transfer Requires Liver- and Muscle-Targeted GDE Expression. Mol. Ther. *26*, 890–901.

60. Puzzo, P., Cagin, U., Van Wittenberghe, L., Daniele, N., Guerchet, N., Colella, P., et al. (2018). AAV-Mediated Liver Expression of Secretable GAA Shows Therapeutic Efficacy in Pompe Mice at Low Vector Doses. The American Society of Gene and Cell Therapy (Chicago: ASGCT).

61. Puzzo, F., Cagin, U., Moya-Nilges, M., Van Wittenberghe, L., Daniele, N., Guerchet, N., et al. (2018). Correction of Advanced Pompe Phenotype in Mice with AAV Liver Gene Transfer of Secretable GAA. The American Society of Gene and Cell Therapy (Chicago: ASGCT).

62. Kupershmidt, L., Weinreb, O., Amit, T., Mandel, S., Carri, M.T., and Youdim, M.B. (2009). Neuroprotective and neuritogenic activities of novel multimodal iron-chelating drugs in motor-neuron-like NSC-34 cells and transgenic mouse model of amyotrophic lateral sclerosis. FASEB J. *23*, 3766–3779.

63. Zincarelli, C., Soltys, S., Rengo, G., and Rabinowitz, J.E. (2008). Analysis of AAV serotypes 1-9 mediated gene expression and tropism in mice after systemic injection. Mol. Ther. *16*, 1073–1080.

64. Gray, S.J., Matagne, V., Bachaboina, L., Yadav, S., Ojeda, S.R., and Samulski, R.J. (2011). Preclinical differences of intravascular AAV9 delivery to neurons and glia: a comparative study of adult mice and nonhuman primates. Mol. Ther. *19*, 1058–1069.

65. Inagaki, K., Fuess, S., Storm, T.A., Gibson, G.A., Mctiernan, C.F., Kay, M.A., and Nakai, H. (2006). Robust systemic transduction with AAV9 vectors in mice: efficient global cardiac gene transfer superior to that of AAV8. Mol. Ther. *14*, 45–53.

66. Chai, Z., Zhang, X., Rigsbee, K.M., Wang, M., Samulski, R.J., and Li, C. (2018). Cryoprecipitate augments the global transduction of the adeno-associated virus serotype 9 after a systemic administration. J. Control. Release *286*, 415–424.

67. Tkach, M., and Théry, C. (2016). Communication by Extracellular Vesicles: Where We Are and Where We Need to Go. Cell *164*, 1226–1232.

68. Han, S.O., Ronzitti, G., Arnson, B., Leborgne, C., Li, S., Mingozzi, F., and Koeberl, D. (2017). Low-Dose Liver-Targeted Gene Therapy for Pompe Disease Enhances Therapeutic Efficacy of ERT via Immune Tolerance Induction. Mol. Ther. Methods Clin. Dev. *4*, 126–136.

69. Xu, L., Mei, M., Haskins, M.E., Nichols, T.C., O'donnell, P., Cullen, K., Dillow, A., Bellinger, D., and Ponder, K.P. (2007). Immune response after neonatal transfer of a human factor IX-expressing retroviral vector in dogs, cats, and mice. Thromb. Res. *120*, 269–280.

70. Wang, G., Miyahara, Y., Guo, Z., Khattar, M., Stepkowski, S.M., and Chen, W. (2010). "Default" generation of neonatal regulatory T cells. J. Immunol. *185*, 71–78.

71. Hinderer, C., Bell, P., Louboutin, J.P., Zhu, Y., Yu, H., Lin, G., Choa, R., Gurda, B.L., Bagel, J., O'Donnell, P., et al. (2015). Neonatal Systemic AAV Induces Tolerance to CNS Gene Therapy in MPS I Dogs and Nonhuman Primates. Mol. Ther. *23*, 1298–1307.

72. Tay, S.S., Wong, Y.C., McDonald, D.M., Wood, N.A., Roediger, B., Sierro, F., Mcguffog, C., Alexander, I.E., Bishop, G.A., Gamble, J.R., et al. (2014). Antigen expression level threshold tunes the fate of CD8 T cells during primary hepatic immune responses. Proc. Natl. Acad. Sci. USA *111*, E2540–E2549.

73. Miyake, N., Miyake, K., Yamamoto, M., Hirai, Y., and Shimada, T. (2011). Global gene transfer into the CNS across the BBB after neonatal systemic delivery of single-stranded AAV vectors. Brain Res. *1389*, 19–26.

74. Manno, C.S., Chew, A.J., Hutchison, S., Larson, P.J., Herzog, R.W., Arruda, V.R., Tai, S.J., Ragni, M.V., Thompson, A., Ozelo, M., et al. (2003). AAV-mediated factor IX gene transfer to skeletal muscle in patients with severe hemophilia B. Blood *101*, 2963–2972.

75. Foust, K.D., Nurre, E., Montgomery, C.L., Hernandez, A., Chan, C.M., and Kaspar, B.K. (2009). Intravascular AAV9 preferentially targets neonatal neurons and adult astrocytes. Nat. Biotechnol. *27*, 59–65.

76. Flanigan, K.M., Campbell, K., Viollet, L., Wang, W., Gomez, A.M., Walker, C.M., and Mendell, J.R. (2013). Anti-dystrophin T cell responses in Duchenne muscular dystrophy: prevalence and a glucocorticoid treatment effect. Hum. Gene Ther. *24*, 797–806.

77. Ramos, J., and Chamberlain, J.S. (2015). Gene Therapy for Duchenne muscular dystrophy. Expert Opin. Orphan Drugs *3*, 1255–1266.

78. Doerfler, P.A., Todd, A.G., Clément, N., Falk, D.J., Nayak, S., Herzog, R.W., and Byrne, B.J. (2016). Copackaged AAV9 Vectors Promote Simultaneous Immune Tolerance and Phenotypic Correction of Pompe Disease. Hum. Gene Ther. *27*, 43–59.

79. Lee, N.C., Hwu, W.L., Muramatsu, S.I., Falk, D.J., Byrne, B.J., Cheng, C.H., et al. (2018). A Neuron-Specific Gene Therapy Relieves Motor Deficits in Pompe Disease Mice. Mol. Neurobiol. *55*, 5299–5309.

80. Smalheiser, N.R. (2007). Exosomal transfer of proteins and RNAs at synapses in the nervous system. Biol. Direct *2*, 35.

81. Andrews, N.W. (2000). Regulated secretion of conventional lysosomes. Trends Cell Biol. *10*, 316–321.

82. Porro, F., Bortolussi, G., Barzel, A., De Caneva, A., Iaconcig, A., Vodret, S., Zentilin, L., Kay, M.A., and Muro, A.F. (2017). Promoterless gene targeting without nucleases rescues lethality of a Crigler-Najjar syndrome mouse model. EMBO Mol. Med. *9*, 1346–1355.

83. Yang, Y., Wang, L., Bell, P., McMenamin, D., He, Z., White, J., Yu, H., Xu, C., Morizono, H., Musunuru, K., et al. (2016). A dual AAV system enables the Cas9-mediated correction of a metabolic liver disease in newborn mice. Nat. Biotechnol. *34*, 334–338.

84. Li, H., Haurigot, V., Doyon, Y., Li, T., Wong, S.Y., Bhagwat, A.S., Malani, N., Anguela, X.M., Sharma, R., Ivanciu, L., et al. (2011). In vivo genome editing restores haemostasis in a mouse model of haemophilia. Nature *475*, 217–221.

85. Barzel, A., Paulk, N.K., Shi, Y., Huang, Y., Chu, K., Zhang, F., Valdmanis, P.N., Spector, L.P., Porteus, M.H., Gaensler, K.M., and Kay, M.A. (2015). Promoterless gene targeting without nucleases ameliorates haemophilia B in mice. Nature *517*, 360–364.

86. Greig, J.A., Nordin, J.M.L., Draper, C., Bell, P., and Wilson, J.M. (2018). AAV8 Gene Therapy Rescues the Newborn Phenotype of a Mouse Model of Crigler-Najjar. Hum. Gene Ther. *29*, 763–770.

87. Hinderer, C., Katz, N., Buza, E.L., Dyer, C., Goode, T., Bell, P., Richman, L.K., and Wilson, J.M. (2018). Severe Toxicity in Nonhuman Primates and Piglets Following High-Dose Intravenous Administration of an Adeno-Associated Virus Vector Expressing Human SMN. Hum. Gene Ther. *29*, 285–298.

88. van der Loo, J.C., and Wright, J.F. (2016). Progress and challenges in viral vector manufacturing. Hum. Mol. Genet. *25* (R1), R42–R52.

89. Hurlbut, G.D., Ziegler, R.J., Nietupski, J.B., Foley, J.W., Woodworth, L.A., Meyers, E., Bercury, S.D., Pande, N.N., Souza, D.W., Bree, M.P., et al. (2010). Preexisting immunity and low expression in primates highlight translational challenges for liver-directed AAV8-mediated gene therapy. Mol. Ther. *18*, 1983–1994.

90. Chan, J., Desai, A.K., Kazi, Z.B., Corey, K., Austin, S., Hobson-Webb, L.D., Case, L.E., Jones, H.N., and Kishnani, P.S. (2017). The emerging phenotype of late-onset Pompe disease: A systematic literature review. Mol. Genet. Metab. *120*, 163–172.

91. Nathwani, A.C., Tuddenham, E.G., Rangarajan, S., Rosales, C., McIntosh, J., Linch, D.C., Chowdary, P., Riddell, A., Pie, A.J., Harrington, C., et al. (2011). Adenovirus-associated virus vector-mediated gene transfer in hemophilia B. N. Engl. J. Med. *365*, 2357–2365.

92. Kodippili, K., Hakim, C.H., Pan, X., Yang, H.T., Yue, Y., Zhang, Y., Shin, J.H., Yang, N.N., and Duan, D. (2018). Dual AAV Gene Therapy for Duchenne Muscular Dystrophy with a 7-kb Mini-Dystrophin Gene in the Canine Model. Hum. Gene Ther. *29*, 299–311.

93. Samaranch, L., Salegio, E.A., San Sebastian, W., Kells, A.P., Foust, K.D., Bringas, J.R., Lamarre, C., Forsayeth, J., Kaspar, B.K., and Bankiewicz, K.S. (2012). Adeno-associated virus serotype 9 transduction in the central nervous system of nonhuman primates. Hum. Gene Ther. *23*, 382–389.

94. Ronzitti, G., Bortolussi, G., van Dijk, R., Collaud, F., Charles, S., Leborgne, C., Vidal, P., Martin, S., Gjata, B., Sola, M.S., et al. (2016). A translationally optimized AAV-UGT1A1 vector drives safe and long-lasting correction of Crigler-Najjar syndrome. Mol. Ther. Methods Clin. Dev. *3*, 16049.

95. Raben, N., Nagaraju, K., Lee, E., Kessler, P., Byrne, B., Lee, L., LaMarca, M., King, C., Ward, J., Sauer, B., and Plotz, P. (1998). Targeted disruption of the acid alpha-glucosidase gene in mice causes an illness with critical features of both infantile and adult human glycogen storage disease type II. J. Biol. Chem. *273*, 19086–19092.